

The Pennsylvania State University

The Graduate School

Department of Geosciences

**STABLE ISOTOPE AND LIPID SIGNATURES OF PLANTS  
ACROSS A CLIMATE GRADIENT: IMPLICATIONS  
FOR BIOMARKER-BASED PALEOCLIMATE RECONSTRUCTIONS**

A Thesis in

Geosciences

by

Christine E. Doman

© 2015 Christine E. Doman

Submitted in Partial Fulfillment  
of the Requirements  
for the Degree of

Master of Science

August 2015

The thesis of Christine E. Doman was reviewed and approved\* by the following:

Katherine H. Freeman  
Professor of Geoscience  
Thesis Advisor

Mark Patzkowsky  
Professor of Geosciences

Matthew Fantle  
Associate Professor of Geosciences

Demian Saffer  
Professor of Geosciences  
Interim Associate Head of Graduate Programs

\*Signatures are on file in the Graduate School

### ABSTRACT

Plant wax *n*-alkanes are long, saturated hydrocarbons that form part of the protective, waxy cuticle on leaves. These lipids are pervasive and persistent in soils and sediments and are ideal biomarkers of ancient terrestrial organic matter. In ecosystems dominated by C<sub>3</sub> plants, fractionation of carbon and hydrogen isotopes during production of whole leaves and hydrocarbon lipids are well documented, but the sensitivity of isotopic fractionation between leaves and lipids to climate has not been fully investigated. Further, there are few studies of stable isotopes in C<sub>4</sub> plant lipids. In both cases, it is unclear if carbon and hydrogen isotopic fractionations during lipid production are sensitive to environmental conditions, such as moisture, or if they reflect inherited characteristics tied to taxonomic or phylogenetic affiliation. This study used a natural climate gradient on the Kohala peninsula of Hawaii to investigate relationships between climate and the  $\delta^{13}\text{C}$  and  $\delta^2\text{H}$  values of *n*-alkanes in three taxa of C<sub>3</sub> and two taxa of C<sub>4</sub> plants.

At Kohala,  $\delta^{13}\text{C}$  values of C<sub>3</sub> plant leaves and lipids decreased 5‰ from the driest to the wettest sites, consistent with published data. As expected, the carbon isotopic composition of C<sub>4</sub> leaves varied less than 2.2‰ for sites that received less than 1060 mm mean annual precipitation (MAP). At sites above 1060 mm MAP, C<sub>4</sub> leaf  $\delta^{13}\text{C}$  values were depleted by up to 15‰ compared to drier sites. This is likely due to shade-related carbon leakage from photosynthetic cells (which can result in a 5-10‰ depletion in  $\delta^{13}\text{C}$ ), possibly enhanced by the influence of a forest canopy at the very wettest site. Biomass  $\delta^{13}\text{C}$  values are lower under a closed canopy where understory plants fix carbon from  $^{13}\text{C}$  depleted, previously respired CO<sub>2</sub>. The combination of these two factors could account for the unusually depleted leaf and lipid carbon isotope values observed at the wettest Kohala sites.

In all C<sub>3</sub> plants and in buffel grass, carbon isotopic fractionation between leaves and lipids ( $^{13}\epsilon_{\text{lipid}}$ ) ranged between 5‰ and 8‰, and did not vary with MAP. In the C<sub>4</sub> Kikuyu grass,

$\epsilon_{\text{lipid}}^{13}$  was consistently lower, between 8 and 10‰, although it was more variable for samples from exceptionally wet sites. Estimates of leaf  $\delta^{13}\text{C}$  for  $\text{C}_3$  and for  $\text{C}_4$  plants below 1060 mm MAP derived from analyses of alkanes preserved in ancient sediments are not sensitive to climate. The apparent fractionation of carbon isotopes in leaves and lipids is sensitive to differences among plant functional type and species.

Hydrogen isotopic values of *n*-alkanes from all plant types did not vary with MAP, but differed consistently between plant functional types and sampled taxa. The absence of a strong trend between fractionation and aridity supports the use of  $\delta^2\text{H}_{\text{lipid}}$  as a record of environmental waters at the time of lipid synthesis, provided that the relative contributions of each plant functional type can be identified with other proxies.

**TABLE OF CONTENTS**

<b>List of Figures .....</b>	<b>vi</b>
<b>List of Tables.....</b>	<b>vii</b>
<b>Awknowlegments.....</b>	<b>viii</b>
<b>Introduction .....</b>	<b>1</b>
<b>Methods .....</b>	<b>11</b>
<b>Results.....</b>	<b>18</b>
<b>Discussion .....</b>	<b>35</b>
<b>Conclusions .....</b>	<b>48</b>
<b>Appendix A: Tables .....</b>	<b>50</b>
<b>Appendix B: Supplemental Figures and Data .....</b>	<b>63</b>
<b>References .....</b>	<b>68</b>

## LIST OF FIGURES

Figure 1. Simplified diagram of C <sub>3</sub> , C <sub>4</sub> , and CAM photosynthesis Modified from Lara and Andreo, 2007.....	6
Figure 2. Expected leaf and lipid δ <sup>13</sup> C values with precipitation for C <sub>3</sub> and C <sub>4</sub> plants, with expected consistent <sup>13</sup> ε <sub>lipid</sub> (McInerney et al., 2013) .....	8
Figure 3. Prevailing Trade winds and 1000 m of elevation change at the Kohala peninsula results in a large gradient in mean annual precipitation (MAP) and mean annual temperature (MAT) across the slope. Sites C-J are located in the rain shadow while site M is located on the windward and rainy side of the ridge. Map at right from Chadwick et al., 2003.....	13
Figure 4. Quantities of <i>n</i> -alkanes per gram TOC per odd length alkanes C <sub>24</sub> -C <sub>33</sub> . Clover sample from site H resembled clover from site M, and is not shown. Buffel grass from site F resembled buffel grass from site E and is not shown. At sites I and M, data shown are averages of multiple specimens of the same species.....	19
Figure 5. Average chain length calculated using C <sub>27</sub> -C <sub>33</sub> for each taxa as a function of precipitation. Linear regressions shown are significant at the p<0.05 level. ....	20
Figure 6. Boxplots of average chain length of individual species. Each box denotes the 25 <sup>th</sup> to the 75 <sup>th</sup> percentile the whiskers extend to the most extreme data point which is no more than 1.5 times the length of the box away from the box. ....	21
Figure 7. δ <sup>13</sup> C values for leaf tissue along the precipitation gradient. Linear regressions shown are significant at the p<0.05 level.....	23
Figure 8. δ <sup>13</sup> C of leaves (filled circles), and lipids, C <sub>27</sub> (open circles), C <sub>29</sub> (open triangles), and C <sub>31</sub> (open squares) along the precipitation gradient. ....	24
Figure 9. <sup>13</sup> ε <sub>lipid</sub> fractionation between leaf δ <sup>13</sup> C and lipid δ <sup>13</sup> C along the precipitation gradient. Note that in C <sub>29</sub> , <sup>13</sup> ε <sub>lipid</sub> of the tree sample from site E (570mm MAP) is the same as the value for the ragwort at that site. Linear regressions shown are significant a p<0.05 level. ....	25
Figure 10. Boxplots of <sup>13</sup> ε <sub>lipid</sub> of C <sub>27</sub> for each sampled species combined from all sites. Each box denotes the 25 <sup>th</sup> to the 75 <sup>th</sup> percentile the whiskers extend to the most extreme data point which is no more than 1.5 times the length of the box away from the box.....	27
Figure 11. δ <sup>2</sup> H of lipids, C <sub>27</sub> (open circles), C <sub>29</sub> (open triangles), and C <sub>31</sub> (open squares) and three models of δ <sup>2</sup> H of precipitation, Bowen and Revenaugh (2003) (solid line), Scholl et al (1995), trade winds area (dotted line), and Scholl et al. (1995) rain shadow area (dashed line). ....	28

- Figure 12.  $^2\epsilon_{\text{lipid}}$  fractionation between modeled  $\delta^2\text{H}$  of precipitation (from Bowen and Revenaugh 2003) and  $\delta^2\text{H}_{\text{lipid}}$  along the precipitation gradient. Linear regressions shown are significant at the  $p < 0.05$  level.....30
- Figure 13. Boxplots of measured  $^2\epsilon_{\text{lipid}}$  by PFT. Gray boxes represent  $^2\epsilon_{\text{lipid}}$  ranges identified by Magill et al., (2013).  $\text{C}_4$  grasses  $-146\text{‰} \pm 8\text{‰}$ ,  $\text{C}_3$  herbs:  $-124\text{‰} \pm 10\text{‰}$ ;  $\text{C}_3$  woody plants:  $-109\text{‰} \pm 8\text{‰}$ ; and  $\text{C}_3$  shrubs:  $-87\text{‰} \pm 4\text{‰}$ , dark grey. Each box denotes the 25<sup>th</sup> to the 75<sup>th</sup> percentile the whiskers extend to the most extreme data point which is no more than 1.5 times the length of the box.....31
- Figure 14.  $^{13}\epsilon_{\text{lipid}}$  and  $^2\epsilon_{\text{lipid}}$  of  $\text{C}_{27}$ ,  $\text{C}_{29}$ , and  $\text{C}_{31}$ .....32
- Figure 15,  $^2\epsilon_{\text{lipid}}$  and  $^{13}\epsilon_{\text{lipid}}$  of  $\text{C}_{29}$  for  $\text{C}_3$  and  $\text{C}_4$  plants from Chikaraishi and Naraoka, 2003; Bi et al., 2005; Smith and Freeman, 2006; Krull et al., 2006 and Kohala samples from this study. Linear regression of  $\text{C}_3$  plants is significant at the  $p < 0.05$  level.....33
- Figure 16.  $^2\epsilon_{\text{lipid}}$  and  $^{13}\epsilon_{\text{lipid}}$  of  $\text{C}_{29}$  for herbs, grasses and trees from Chikaraishi and Naraoka, 2003; Bi et al., 2005; Smith and Freeman, 2006; Krull et al., 2006 and Kohala samples from this study. None of the regressions were significant at the  $p < 0.05$  level.....34

## LIST OF TABLES

Table 1. Climate Variables . Site M is located on the windward and rainy side of the ridge. $\delta^2\text{H}_{\text{precipitation}}$ modeled using Bowen and Revenaugh (2003) (BR), and Scholl et al (1995; 1996) for rain shadow (RS) and trade wind (TW) dominated areas .....	50
Table 2. Linear regressions of total <i>n</i> -alkanes and mean annual precipitation. None of the regressions were significant at the 0.05 level.....	50
Table 3. Quantities of individual <i>n</i> -alkanes in leaf samples. ....	52
Table 4. Average chain length, leaf $\delta^{13}\text{C}$ , $\delta^{13}\text{C}_{\text{lipid}}$ , and $^{13}\epsilon_{\text{lipid}}$ of leaf wax <i>n</i> -alkanes. ACL was calculated using $\text{C}_{27}$ , $\text{C}_{29}$ , $\text{C}_{31}$ , and $\text{C}_{33}$ . ....	53
Table 5. Linear regression of ACL and mean annual precipitation. P-values in bold italics are significant at the 0.05 level. ....	54
Table 6. Linear regression of $\delta^{13}\text{C}_{\text{leaf}}$ and mean annual precipitation. P-values in bold italics are significant at the 0.05 level.....	55
Table 7. Linear regression of $^{13}\epsilon_{\text{lipid}}$ values and mean annual precipitation. P-values in bold italics are significant at the 0.05 level.....	56
Table 8. $\delta^2\text{H}_{\text{‰}}$ VSMOW of precipitation modeled after Bowen and Revenaugh (2003) , measured $\delta^2\text{H}_{\text{lipid}}$ and $^2\epsilon_{\text{lipid}}$ of leaf wax <i>n</i> -alkanes. ....	57
Table 9. Linear regressions of $^2\epsilon_{\text{lipid}}$ values and mean annual precipitation. P-values in bold italics are significant at the 0.05 level.....	58
Table 10. Linear regressions of $\delta^{13}\text{C}$ and $^2\epsilon_{\text{lipid}}$ . P-values in bold italics are significant at the 0.05 level. ....	59
Table 11. Linear regressions of $^{13}\epsilon_{\text{lipid}}$ and $^2\epsilon_{\text{lipid}}$ . P-values in bold italics are significant at the 0.05 level. ....	60



## ACKNOWLEDGEMENTS

This thesis has my name on it but many thanks are due to others before you can continue reading. Thanks are due to my steadfast adviser Kate Freeman and our lab's technical wizard Denny Walizer without whom nothing would ever get done and everything would always be broken. I would like to thank Sarah Enders and Oliver Chadwick for collecting these samples in 2011. Laura Fontanills deserves credit for beginning the lab work for this project and grinding many, many bags of dry grass. I would also like to thank my fellow students who have gone on ahead of me Clay Magill and Heather Graham, as well as those who shared bench space and syringes, Elizabeth Denis, Laurence Bird, Angela Chung Laura Herren, and my former undergraduate helper Annie Tamalavage.

I must also thank my parents Mark Doman and Jane Allen and my sister Genevieve Doman for politely listening to me complain, and smiling and nodding when I try to explain what it is that I have done.

## Introduction

As biomarkers, fossil molecules from plants can provide high-resolution reconstructions of past climate (Hayes et al., 1990; Freeman and Colarusso, 2001; Schwark et al., 2002; Boot et al., 2006; Hren et al., 2010; Tipple and Pagani, 2010; Galy et al., 2011). As living things incorporate carbon and hydrogen into their tissues, their isotopic compositions preserve a record of environmental conditions. But first, biomarkers must be studied in modern environments to understand what, if any, information can be preserved in the geologic record.

*n*-alkanes, straight chain, saturated hydrocarbons are frequently used as biomarkers of plant cover in the geologic record (Pancost et al., 2013; Sun et al., 2013; Lopes dos Santos et al., 2013; Leider et al., 2013). Alkanes of odd chain lengths between C<sub>25</sub> and C<sub>35</sub> are generally attributed to terrestrial higher plants (Eglinton and Hamilton, 1967), and specifically angiosperms (Diefendorf et al., 2011; Diefendorf et al., 2014). The presence of longer chains, including C<sub>33</sub> and C<sub>35</sub>, are considered to be indicative of C<sub>4</sub> grass contribution to (Vogts et al., 2012; Bush and McInerney, 2013; Henderson et al., 2014; Bush and Mcinerney, 2015). The  $\delta^{13}\text{C}$  values of total organic carbon (TOC) in sediments represent contributions from C<sub>3</sub> vs. C<sub>4</sub> plants, but this interpretation cannot be used when there are other sources of carbon or diagenetic alteration of TOC (Meyers and Ishiwatari, 1993). The carbon and hydrogen isotope ratios of individual *n*-alkanes derived from plant leaves can be measured directly to avoid conflating terrestrial and non-terrestrial carbon in sediment (Freeman and Colarusso, 2001).

Isotopic fractionation between the leaf and lipid carbon is often assumed to be constant regardless of climate conditions, but this has not been directly studied and the assumption has recently been questioned (McInerney et al., 2013). The interplay between climate and plant communities complicates interpretation of isotope and abundance data for *n*-alkanes in sediments.

In order to better constrain the climate signals recorded in sedimentary alkanes, it is necessary to investigate their behavior in modern environments.

The Kohala peninsula of Hawaii is uniquely situated to investigate the effects of climate on leaf waxes. The leeward side of the peninsula sits in a rain shadow and experiences a broad range of climate conditions from the shore to the top of the ridge. Only a small number of plant species exist along the gradient, which can be sampled across strongly variable climate conditions. Similar studies are often hampered by the fact that plant communities change with along such a broad climate gradient. At Kohala, a small number of species are present in a range of climate conditions making the peninsula a natural laboratory to investigate the effect of climate on carbon and hydrogen isotopic fractionation in both C<sub>3</sub> and C<sub>4</sub> plants.

### **Leaf waxes**

*n*-Alkanes make up part of the waxy cuticle that forms the outermost protective layer of a leaf. Epicuticular wax is a mixture of *n*-alkanes and *n*-alkanolic acids which form a cross-linked mesh across the surface of the leaf (Eglinton et al., 1962). Early researchers identified an odd-over-even pattern in the lengths of *n*-alkane chains (Albert et al., 1934) and noted taxonomic patterns in the lengths and quantities of these molecules (Eglinton et al., 1962).

The exact function of the waxes is still up for debate. Leaf waxes scatter UV light to protect plants from overheating (Eglinton and Hamilton, 1967). They provide some structure and plasticity to the leaf surface (Domínguez et al., 2011) and protect from fungal attack (Bourdenx et al., 2011). The network of long chain alkanes and acids traps water vapor to create an insulating layer of humidity to reduce water loss by evapotranspiration (Kerstiens, 1996). This hypothesis is bolstered by evidence that water-stressed plants produce more and longer alkanes than well watered specimens (Rao et al., 1996; Macková et al., 2013). The quantity of *n*-alkanes produced

also varies by leaf type (sun vs. shade) (Feng, 1999), plant type (Carr et al., 2014) and taxonomy (Diefendorf et al., 2011).

Most of these studies focus on *n*-alkane amounts in C<sub>3</sub> plants, despite the fact that C<sub>4</sub> grasslands have been a globally important plant group since the late Miocene and cover 20% of land today (Cerling et al., 1997; Freeman and Colarusso, 2001; Edwards et al., 2010; Scheiter et al., 2012). This lack of research limits our ability to interpret paleorecords of leaf waxes sourced from C<sub>4</sub>-dominated ecosystems. How the carbon and hydrogen isotopes of C<sub>4</sub> grasses change—or do not change—with climate is not clear in published research, but it is vital to understand the global history of the grassland biome.

### **Average Chain Length**

The average chain length (ACL) of leaf wax *n*-alkanes is frequently used in paleoclimate reconstructions (Boot et al., 2006; Rommerskirchen et al., 2006a; Tipple and Pagani, 2010; Sun et al., 2013). Plants produce variable quantities of each odd alkane C<sub>25</sub>-C<sub>35</sub> depending on plant type. For example, succulents produce more alkanes than herbs or woody plants, and their contribution to sedimentary alkanes can overwhelm the signal from other plants (Boom et al., 2014; Carr et al., 2014). Similarly, grasses tend to produce longer chain lengths, but much less leaf wax, than woody plants (Rommerskirchen et al., 2006; Vogts et al., 2012). Because of this, all grasses tend to be underrepresented in sedimentary alkane records. Within a species, ACL appears to increase with temperature (Maffei, 1996; Sachse et al., 2006; Bush and McInerney, 2013; Carr et al., 2014; Bush and McInerney, 2015), which suggests longer alkane chains help regulate temperature or combat water stress. Chain length is influenced primarily by taxonomy, and in part by environment.

Few publications document ACL in C<sub>4</sub> grasses (Maffei, 1996; Rommerskirchen, Plader, et al., 2006; Vogts et al., 2012; Bush and McInerney, 2013; Bush and Mcinerney, 2015), especially in response to changes in climate. In this study, we sampled plants at Kohala along a natural climate gradient to investigate the effects of climate on leaf wax attributes.

### **Photosynthetic Pathways**

Most plants use the Calvin-Benson cycle to convert carbon from CO<sub>2</sub> to sugars via 3-phosphogluconate, a three carbon acid intermediate, hence the appellation C<sub>3</sub> photosynthesis (Bassham et al., 1950). In C<sub>3</sub> plants, stomatal pore cells are open during photosynthesis to allow for the diffusion of CO<sub>2</sub> into and O<sub>2</sub> out of the leaf. Because stomata also allow water loss from the leaf interior, C<sub>3</sub> plants must close their stomata and cease photosynthesis under hot or dry conditions. At high temperatures, photooxidation reduces the efficiency of C<sub>3</sub> photosynthesis by as much as 25% (Percy and Ehleringer, 1984; Farquhar et al., 1989; Ehleringer et al., 1991). As a result, hot and dry environments limit the photosynthetic efficiency of C<sub>3</sub> plants (Percy and Ehleringer, 1984; Farquhar et al., 1989; Sage, 2004).

More than 60 distinct clades of plants use the C<sub>4</sub> photosynthetic pathway, which reduces water loss and photooxidation (Edwards and Smith, 2010). To prevent photooxidation, RuBisCo—ribulose-bisphosphate carboxylase, the enzyme that facilitates carbon fixation—is isolated from O<sub>2</sub> in modified bundle-sheath cells. CO<sub>2</sub> is transported to the bundle-sheath cells via the four-carbon acid, malate (Figure 1), which gives C<sub>4</sub> plants their name. The physical separation of gas exchange and photosynthesis allows the plant to fix carbon with closed stomata. These adaptations give C<sub>4</sub> plants an advantage in warm, dry environments and at low atmospheric CO<sub>2</sub> concentrations (Farquhar et al., 1989; Ehleringer et al., 1991; Pau et al., 2013; Teeri et al., 2014). C<sub>4</sub> plants are generally at a disadvantage in low light conditions (Percy and Ehleringer,

1984; Ehleringer et al., 1991; Vogan and Sage, 2012) where the absorption of CO<sub>2</sub> into the cell can outpace the fixation of carbon, resulting in leakage of CO<sub>2</sub> from bundle-sheath cells and a reduction in photosynthetic efficiency (Sage and McKown, 2006; Sage, 2014). As a result of evolution and physiology, C<sub>4</sub> grasses outcompete their C<sub>3</sub> counterparts in dry, high light environments

The anatomical and biochemical differences between C<sub>3</sub> and C<sub>4</sub> plants result in diagnostically different carbon isotope fractionation between the two. In C<sub>3</sub> plants, <sup>12</sup>C is preferentially incorporated in plant cells due to diffusion of CO<sub>2</sub> into the leaf and the isotopic fractionation associated with the carbon fixing enzyme RuBisCo (O'Leary, 1981; O'Leary, 1988). C<sub>4</sub> plants use RuBioCo as well, but different carboxylases and the internal transportation of CO<sub>2</sub> result in a far lower degree of mass sensitivity (Ehleringer et al., 1991; Ehleringer et al., 1997). The different uptake of <sup>13</sup>C in C<sub>3</sub> and C<sub>4</sub> plants causes characteristic differences in the carbon isotopes of their respective plant tissues. C<sub>3</sub> plants are depleted in <sup>13</sup>C, with leaf δ<sup>13</sup>C values that range between -35‰ to -20‰. C<sub>4</sub> plants are more enriched in <sup>13</sup>C and have a narrower range of δ<sup>13</sup>C values, usually between -10‰ to -16‰ (Cerling et al., 1997).

The difference in variability is due to the two photosynthetic pathways. Stomata of C<sub>3</sub> plants open more under wet conditions, where the fractionation due to diffusion and RuBisCo result in lower carbon isotope values. Under dry conditions, stomata are closed more, which leads to higher values. In C<sub>4</sub> plants, photosynthesis continues independently of open or closed stomata, and the range of fractionation is smaller (Farquhar et al., 1989). In low-light conditions, C<sub>4</sub> plants with leaky photosynthesis can have 5‰ to 10‰ more depleted carbon isotope values than the same plants in high light environments (Sage and McKown, 2006; Lanigan et al., 2008; Ubierna et al., 2013; Bellasio and Griffiths, 2014; Sage, 2014).

The natural laboratory at Kohala allowed C<sub>3</sub> and C<sub>4</sub> plants to be sampled at the same sites along a climate gradient. The two photosynthetic pathways can be directly compared in plants

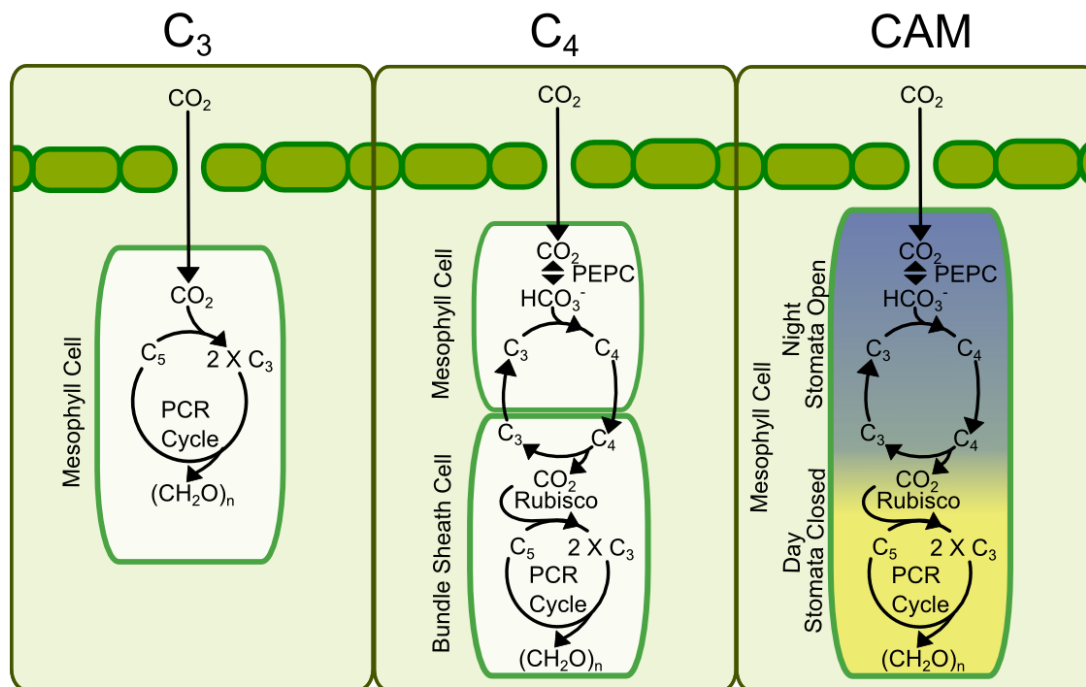


Figure 1. Simplified diagram of  $C_3$ ,  $C_4$ , and CAM photosynthesis Modified from Lara and Andreo, 2007.

in the same conditions. If carbon or hydrogen isotope fractionation is influenced by climate in either type of plant, this data set should be able to detect it.

### **Isotopic Fractionation between whole leaf and leaf wax isotopes**

The offset between the leaf and lipid isotopic values is presumed to be consistent across varying climates (Figure 2.) (Collister et al., 1994; Chikaraishi et al., 2004; Diefendorf et al., 2010; McInerney et al., 2013; Magill et al., 2013a), yet  $^{13}\epsilon_{\text{lipid}}$  has been measured and compared to available moisture in only a few cases (Wei and Jia, 2009; McInerney et al., 2013). The fractionation between leaf and lipid carbon isotopes has important bearing on interpretations carbon isotope excursions (CIE) in the past. CIEs are evidence for large-scale perturbations to the carbon cycle. Most notably, the Paleocene-Eocene Thermal Maximum (PETM) is marked by a  $\sim 3\text{‰}$  decrease in  $\delta^{13}\text{C}$  of total organic carbon, but alkane records report excursions of  $\sim 4\text{-}5\text{‰}$  (Smith et al., 2007). The reason for the difference between the CIE in the two types of records is have been debated (Schouten et al., 2007; Smith et al., 2007; Zachos et al., 2010). Most interpretations of lipid records assume that the fractionation between carbon in leaves and lipids ( $^{13}\epsilon_{\text{lipid}}$ ) is invariable with climate. Yet, this assumption has never been tested directly. If  $^{13}\epsilon_{\text{lipid}}$  does vary with climate, then the CIE expressed by alkanes would reflect local conditions in addition to global changes in the  $\delta^{13}\text{C}$  of  $\text{CO}_2$ . Understanding how climate does or does not affect  $^{13}\epsilon_{\text{lipid}}$  would clarify how well the PETM isotope excursion in alkane records captures global changes in atmospheric carbon isotopes (Gröcke, 2002; Smith et al., 2007).

In this study, I take advantage of a small set of species sampled across a broad natural climate gradient to determine how  $^{13}\epsilon_{\text{lipid}}$  is related to aridity and temperature. It will provide a dataset that will examine whether taxonomy or environment has a greater effect on the fractionation of carbon in leaf wax lipids.



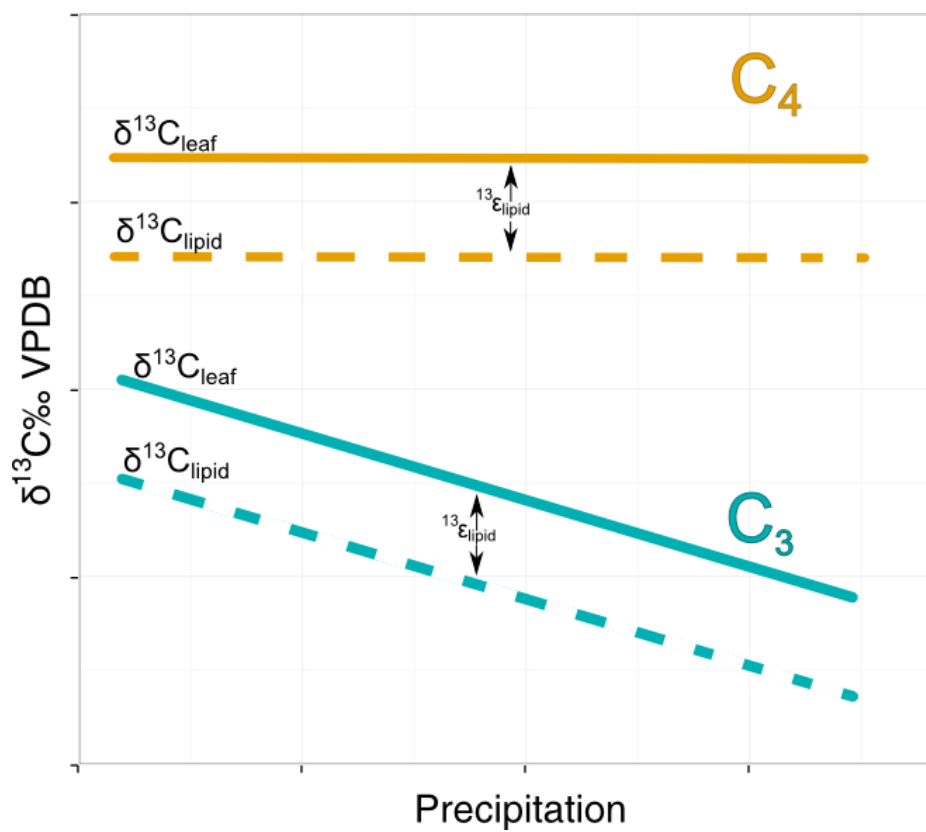


Figure 2. Expected leaf and lipid  $\delta^{13}\text{C}$  values with precipitation for  $\text{C}_3$  and  $\text{C}_4$  plants, with expected consistent  $^{13}\epsilon_{\text{lipid}}$  (McInerney et al., 2013).

## Hydrogen Isotopes of Leaf Wax Lipids

The hydrogen isotope ratios of leaf wax lipids are controlled by environmental waters and by mass sensitivity during biosynthesis, which incorporates hydrogen into lipids via NADPH+ (McInerney et al., 2011; Sachse et al., 2012). The source of hydrogen is plant water, which is itself fractionated by evaporation from soils prior to root uptake. Hydrogen isotopes are not fractionated when water is absorbed by roots (Ehleringer and Dawson, 1992), but leaf water becomes enriched in  $^2\text{H}$  as water is drawn out of the leaf by evapotranspiration. Hydrogen isotopes are used to trace the source of water used by plants and to estimate evapotranspiration (Dawson, 1996; Darrouzet-nardi et al., 2006). Fractionation of hydrogen isotopes in soil water, leaf water and leaf lipids is controlled by the environment and functional type of plant (Magill et al., 2013b).

$\delta^2\text{H}_{\text{lipid}}$  values from sediments should reflect  $\delta^2\text{H}_{\text{soil}}$  at the time of lipid synthesis because the hydrogen isotope ratios of leaf wax *n*-alkanes of grasses have been shown to be insensitive to transpiration (McInerney et al., 2011). However, this is debated, and how leaf water influences lipid  $\delta^2\text{H}$  is not entirely clear (Polissar and D'Andrea, 2014). Organic matter in sediments is a mixture of compounds that can differ in isotopic composition due to the different biosynthetic pathways and source organisms (Schimmelmann et al., 2006). Because of this, it is difficult to obtain robust paleohydrological records with bulk sedimentary organic matter (Krishnamurthy et al., 1995; Sachse et al., 2012). The isotope ratios of individual alkanes can provide paleoenvironmental information, provided that the fractionation between hydrogen isotopes in water and leaf lipids is understood. The growth habit of a plant influences  $\delta^2\text{H}$  of leaf water by controlling the pool of internal water being fractionated while the photosynthetic pathway governs the amount of evapotranspiration from the leaf. Any environmental signal from  $\delta^2\text{H}_{\text{lipid}}$  from sediments can only be interpreted if the predominant plant functional type of the ecosystem

can be identified. Alkane biomarker metrics including ACL and  $\delta^{13}\text{C}_{\text{lipid}}$  are required to identify the ecosystem and plant cover from sedimentary biomarkers.

Magill et al. (2013b) reconstructed the environment of a 2 million year old East African lake with a combination of carbon isotopes, biomarkers for woody vs non-woody vegetation, salinity proxies, and hydrogen isotopes of *n*-alkanes. The type of vegetation ( $\text{C}_3$  woody,  $\text{C}_3$  herbaceous, or  $\text{C}_4$  grass) was estimated from leaf and lipid  $\delta^{13}\text{C}$  values. The authors were able to estimate the apparent fractionation factor, based on published ranges in apparent hydrogen isotope fractionation in lipids. They then used lipid  $\delta^2\text{H}$  values with epsilon to reconstruct meteoric water isotope patterns. The current study investigates the relationship between aridity and  $^2\varepsilon_{\text{lipid}}$ , as well as contributing measurements of  $^2\varepsilon_{\text{lipid}}$  in tropical grasslands, similar to the ecosystems Magill et al. studied. While  $\text{C}_3$  leaf waxes are well studied, relatively little is known about the leaf wax properties of  $\text{C}_4$  grasses, despite their global importance. It is well known that the carbon isotope value of  $\text{C}_3$  leaves varies with climate (Stewart et al., 1995; Van D Water et al., 2002; Bowling et al., 2002; Ma et al., 2012). Even less is known about the carbon and hydrogen isotopic composition of  $\text{C}_4$  grass leaf waxes in association with climate. To improve applications using leaf waxes to study past plants and climate we must understand the sensitivity of plant wax isotope signatures to climate, ecology and physiological factors. Even more than  $\text{C}_3$  plants, the contribution of  $\text{C}_4$  grass *n*-alkanes to the geologic record needs to be better understood.

The Kohala peninsula of Hawaii provides a natural laboratory where seasonality is limited, and a limited number of species are present in an area that includes both hot and dry, and cold and wet environments. This experiment determines how climate affects carbon or hydrogen isotope fractionation in  $\text{C}_3$  and  $\text{C}_4$  plants.

## Methods

### Site Description

The wide range in rainfall across the Kohala peninsula has been used to study the effects of precipitation on soil development and weathering (Chadwick et al., 2003). Additionally, the disparity in precipitation between the windward and leeward sides of the ridge offer a natural laboratory to study the effects of climate on carbon and hydrogen isotope fractionation in C<sub>4</sub> grasses. Samples were collected by Sarah Enders in 2011 along a transect established by Chadwick et al (2003) across the center of the Kohala peninsula in the north western corner of the Big Island of Hawaii (Figure 3) (Chadwick et al., 2007; Cusack et al., 2012; McCoy et al., 2013).

Weather patterns are dominated by the northeast trade winds, which result in a pronounced rain shadow westward across the ridge. Mean annual precipitation (MAP) across the sample transect range from 210 mm to 1500 mm per year. Year-to-year variation is high, ranging from 700 mm to 1000 mm MAP at mid elevations, depending on cyclone activity. Seasonality is low, with precipitation distributed equally throughout the year (Giambelluca et al., 1986). The sample sites range in elevation from 256 m to 1152 m above sea level, and average temperatures range from 23° to 17°C at the lowest and highest sites. The rain shadow and topography result in warm and dry sites at low elevations, and cold, wet sites at high elevations.

The sites are primarily pastureland and dominated by C<sub>4</sub> grasses introduced to Hawaii with European contact in the 18th century (Wilén and Holt, 1996; Daehler and Goergen, 2005; Ghannoum et al., 2008; Muscolo et al., 2013). Lower elevation sites are dominated by C<sub>4</sub> buffel grass (*Cenchrus ciliaris*) and C<sub>3</sub> American carob trees (*Prosopis pallida*). Upper elevations are dominated by C<sub>4</sub> Kikuyu grass (*Pennisetum clandestinum*), named after the Kikuyu people of East Africa, and C<sub>3</sub> Madagascar ragwort (*Senecio madagascariensis*) a flowering herb, and the

occasional clover (*Trifolium spp.*). At each site, for each species, samples were taken of leaves from each plant present, accumulated leaf litter, and the top 10 cm of soil. The soils are roughly the same age and developed on chemically similar lava flows (Chadwick et al., 2007). Plant samples were collected in the summer of 2011 by Sara Enders working with Dr. Oliver Chadwick at previously established sites (Chadwick et al., 2003). Whole grasses and herb plants—including flowers and seeds—were sampled above the soil level. Several tree leaves were chosen from sun leaves to avoid any shade effects. Leaf litter—undecomposed plant matter—was collected at random within a site. Soil samples were taken from the top 10 cm of soil below the leaf litter. All samples were packed in Whirl-Pak® bags and shipped to Penn State for analysis.

### **Sample Preparation**

All samples were dried using a Labconco Freezone 4.5 freeze dry system and ground using an SPEX 8000 steel ball mill for five minutes. In between samples, the milling container was rinsed with deionized water, methanol, dichloromethane (DCM) and hexane, cleaned by grinding 5 ml of ashed Ottawa sand, and finally rinsed with water and solvents .

Ground samples were extracted and separated using a Dionex Accelerated Solvent Extractor (ASE 200). Total lipid extracts were obtained from ~300 mg plant material, ~500 mg leaf litter, and ~1000 mg soils using 9:1 DCM:methanol. Saturated hydrocarbons were separated following Magill et al. (submitted) using layers of Ottawa sand mixed with diatomaceous earth, silver impregnated alumina, silica gel and 19:1 hexane:DCM. More polar compounds were extracted by inverting the cells and extracting with 4:1 DCM:methanol.

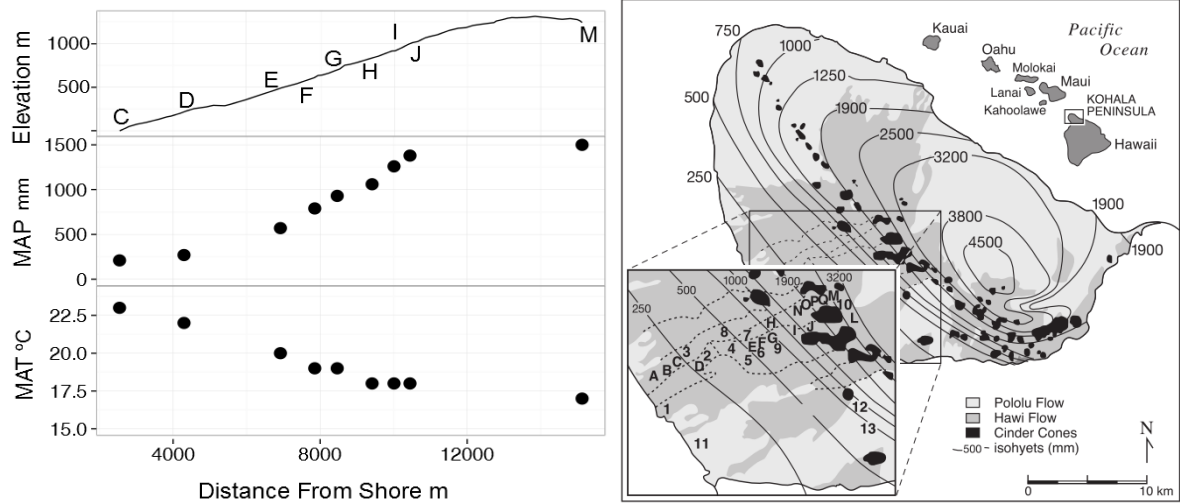


Figure 3. Prevailing Trade winds and 1000 m of elevation change at the Kohala peninsula results in a large gradient in mean annual precipitation (MAP) and mean annual temperature (MAT) across the slope. Sites C-J are located in the rain shadow while site M is located on the windward and rainy side of the ridge. Map at right from Chadwick et al., 2003.

### Alkane characterization

Plant wax alkanes were identified using GC–MS (Hewlett–Packard 6890 GC connected to a HP 5973 quadrupole MS) using electron-impact ionization and a Restek Rxi-5HT fused silica capillary column. Samples were injected in splitless mode using helium as the carrier gas at a flow rate of 2.0 ml/min. The oven temperature was held at 60 °C for 1 minute, increased by 6 °C per minute to 320 °C, and then held for 20 minutes. Pentacosane, heptacosane, nonacosane, hentriacontane, tritriacontane, and pentatriacontane ( $C_{25}$ – $C_{35}$ ) were identified from mass spectra and retention times using standard alkanes of chain lengths  $C_7$ – $C_{38}$ .

*n*-Alkanes were quantified using a HP 5890 gas chromatograph with a flame ionization detector (FID) using a fused silica capillary column (Agilent J&W DB-5; 30m, 0.25mm) coated with (5% -phenyl-methylpolysiloxane 25mm film thickness). Helium was used as the carrier gas at 2.0 ml/min. Starting temperature was 60°C, increased 6°C per minute to 320°C, and held at 320°C for 20 minutes. Samples were run in batches of 7 bracketed by  $C_7$ – $C_{38}$  alkane standards. One was chosen at random and run in the next batch to check reproducibility. Duplicates were 6% different from each other on average. Samples were quantified using response curves for 31 *n*-alkanes ( $C_7$ – $C_{38}$ ) analyzed in concentrations of 10, 20, 50 and 100 µg/µl.  $R^2$  of the response curves for individual alkane (odd alkanes  $C_{25}$ – $C_{35}$ ) averaged 0.985. Plant lipid abundances were normalized to grams total organic carbon as measured by elemental analysis (e.g., µg/g TOC).

Average chain length was calculated using a modified equation from Freeman and Pancost (2014) (equation 1), which is a weighted average of alkane concentration using chain lengths as weights. Although many authors calculate ACL from alkanes  $C_{25}$ – $C_{35}$ , here  $C_{25}$  was excluded because it provides little taxonomic information, and  $C_{35}$  was excluded because it was not detected in any samples (Bush and McInerney, 2013).  $C_{27}$ ,  $C_{29}$ ,  $C_{31}$ , and  $C_{33}$  best represent alkanes which are diagnostic of plant functional type in the geochemical record. The carbon

preference index (CPI) identifies the odd-over-even alkane distribution characteristic of organic terrestrial plants. Because the samples were taken from living plants and have a pronounced odd-over-even preference, CPI is not reported for these samples.

Equation 1

$$ACL = \frac{(27[C_{27}] + 29[C_{29}] + 31[C_{31}] + 33[C_{33}])}{([C_{27}] + [C_{29}] + [C_{31}] + [C_{33}])}$$

### Isotopic analysis

The  $\delta^{13}\text{C}$  values for leaves were measured by combustion in a ThermoFinnigan Delta+ XP elemental analyzer. A suite of isotopic and quantitative standards were used throughout sample runs to establish accuracy following the methods of Coplen et al. (2006). Error was determined by repeated analysis of internal standards of caffeine, glycine USGS-24, sucrose, and lab standard Peru mud. The instrument precision standard deviation was  $\pm 0.18\text{‰}$  ( $n=44$ ). Accuracy was  $0.4\text{‰}$  ( $n=92$ ), calculated as the average difference between measured and known  $\delta^{13}\text{C}$  values of standards of caffeine, glycine, lab standard Peru mud, sucrose, and USGS-24.

Compound-specific  $\delta^{13}\text{C}$  values were measured by a Finnigan MAT 252 isotope ratio monitoring–MS using a Varian gas chromatograph and combustion interface.  $\text{C}_{38}$  and  $\text{C}_{41}$  were used as internal standards throughout sample runs to establish precision and accuracy. For measurements of  $\text{C}_{38}$  and  $\text{C}_{41}$ , accuracy (measured minus known values) ranged between  $0.2\text{‰}$  and  $0.4\text{‰}$ . Precision was determined by repeated analysis of odd carbon chains  $\text{C}_{25}$ – $\text{C}_{35}$  in Schimmelmann standard Mix B ( $\text{C}_{16}$ – $\text{C}_{30}$ ; Arndt Schimmelmann, Indiana University) and was also between  $0.2$  and  $0.4\text{‰}$ .

Compound-specific  $\delta^2\text{H}$  values of *n*-alkanes were measured using an HP 6890 GC connected to a Thermo Finnegan Delta Plus XP IRMS with a combustion interface and a high-



temperature pyrolysis furnace held at 1400°C The daily average  $H_3^+$  factor was recorded throughout the analytical time frame. Isotopic composition is determined relative to a reference gas calibrated to an international standard, as well as by injections of Mix B (n-C16 to n-C30; Arndt Schimmelmann, Indiana University) with known D/H ratios. Isotope values of samples are reported in delta notation relative to Vienna Standard Mean Ocean Water (VSMOW) (Burgoyne and Hayes, 1998; Graham, 2014)

All  $\delta$  values were calculated using standard  $\delta$  notation (equation 2), following Keeling (1958). Carbon isotope values are reported relative to the Vienna Pee-Dee Belemnite (VPDB). Hydrogen isotopes are reported relative to Vienna Standard Mean Ocean Water (VSMOW). The fractionation factors between leaf  $\delta^{13}C$  and leaf lipid  $\delta^{13}C$  ( $^{13}\epsilon_{lipid}$ ) were calculated using Equation 3 following Chikaraishi et al. (2004). The same equation was modified (Equation 4) and used to determine  $^2\epsilon_{lipid}$  using estimated  $\delta^2H$  of precipitation as  $\delta^2H_{water}$ .

Equation 2

$$\delta \text{ ‰} = \left( \frac{R_{sample}}{R_{standard}} - 1 \right) * 1000$$

Equation 3

$$^{13}\epsilon_{lipid} \text{ ‰} = \left[ \frac{\delta^{13}C_{lipid} + 1000}{\delta^{13}C_{leaf} + 1000} - 1 \right] * 1000 \approx \delta^{13}C_{lipid} - \delta^{13}C_{leaf}$$

Equation 4

$$^2\epsilon_{lipid} \text{ ‰} = \left[ \frac{\delta^2H_{lipid} + 1000}{\delta^2H_{water} + 1000} - 1 \right] * 1000 \approx \delta^2H_{lipid} - \delta^2H_{water}$$

### **$\delta^2H$ of precipitation estimations**

Estimated values  $\delta^2H$  of precipitation using the WaterIsotopes.org calculator, following Bowen and Revenaugh (2003), were based on latitude, longitude and altitude to estimate  $\delta^2H$  and

$\delta^{18}\text{O}$  of precipitation. The calculator does not account for local effects, like the rain shadow at Kohala in North West Hawaii. We therefore compared the Bowen and Revenaugh estimates to linear regressions of published  $\delta^2\text{H}$  of precipitation from wet (windward) and dry (leeward) areas for the southwest coast of Hawaii, near Hilo (Scholl et al., 1995; Scholl et al., 1996). The Bowen and Revenaugh (2003) estimates of  $\delta^2\text{H}$  range from -11‰ to -23‰. Estimates based on Scholl et al (1996). for wet areas were similar to Bowen and Revenaugh (2003) (-14‰ to -25‰) but are lower in dry regions (-29‰ to -37‰) (Table 1). Despite its shortcomings, the Bowen and Revenaugh (2003) model has been used in similar studies when direct measurements of precipitation are unavailable (Feakins and Sessions, 2010; Sachse et al., 2012; McInerney et al., 2013; Magill et al., 2013b; Leider et al., 2013).

### **Statistical Analysis**

Linear regressions were calculated using mean annual precipitation (MAP) as the climate variable. Plots of isotopic variables against MAP or MAT show identical trends. Due to the small range in temperature

Linear least squares regressions were calculated using R the linear model function in the standard R package (R Core Team, 2014). Ordinary linear least squares regressions like this assume there is no variation in the explanatory variable, in this case MAP. Mean annual precipitation values were based on a regression of sampled sites and measured precipitation to predict rainfall as a function of elevation with an  $r^2$  of 0.96 (Chadwick et al., 2003). Stepwise multiple linear regressions revealed that no combination of factors (precipitation, temperature, or elevation) together explained any more variability than a single linear regression (Diefendorf, 2010). P-values values for multiple linear regressions were all above 0.05.

## Results

### ***n*-Alkane quantities and Average Chain Length**

The amount of *n*-alkanes decreased with increasing precipitation, for all plant taxa. None of the linear regressions of alkane quantity and MAP for plant taxa, functional type or photosynthetic pathway were significant at the  $p < 0.05$  level.  $C_{29}$  and  $C_{31}$  were the most abundant *n*-alkanes in the leaves of  $C_3$  trees and herbs.  $C_{31}$  and  $C_{33}$  were the most abundant alkanes in  $C_4$  grasses, with  $C_{33}$  more abundant in leaves at the wettest sites. In  $C_3$  plants, the most abundant *n*-alkane was between 50% to 60% more abundant than the next most plentiful alkane (Table 3). In the case of  $C_3$  trees,  $C_{27}$  made up over 15,000 ng/g TOC (Figure 4 Table 3). In  $C_4$  grasses, the quantity of alkanes was typically much lower ( $< 1000$  ng/g TOC) and more evenly distributed by homologue than in  $C_3$  plants.

Average chain length ranged from 26.7 to 30.1 in  $C_3$  plants and 29.5 to 31.2 in  $C_4$  plants (Table 4). ACL was positively correlated with MAP in both  $C_3$  and  $C_4$  grasses (Figure 5, Table 5). At dry sites (200 mm-800 mm MAP), ACL of  $C_4$  Buffel grass remained relatively constant but at wet sites (800 mm-1500 mm MAP), ACL of Kikuyu grass increased markedly (Figure 5, Table 5). At the windward site (site M), ACL of the two coexisting  $C_3$  and  $C_4$  plants were similar, with means of 30.1 for clover, and 29.7 for Kikuyu grass. Carob trees sampled at the two driest sites (C and D) did not contain any alkanes longer than  $C_{27}$ . Plant species had a strong influence on variation in ACL, shown in boxplots of ACL by species (Figure 6).

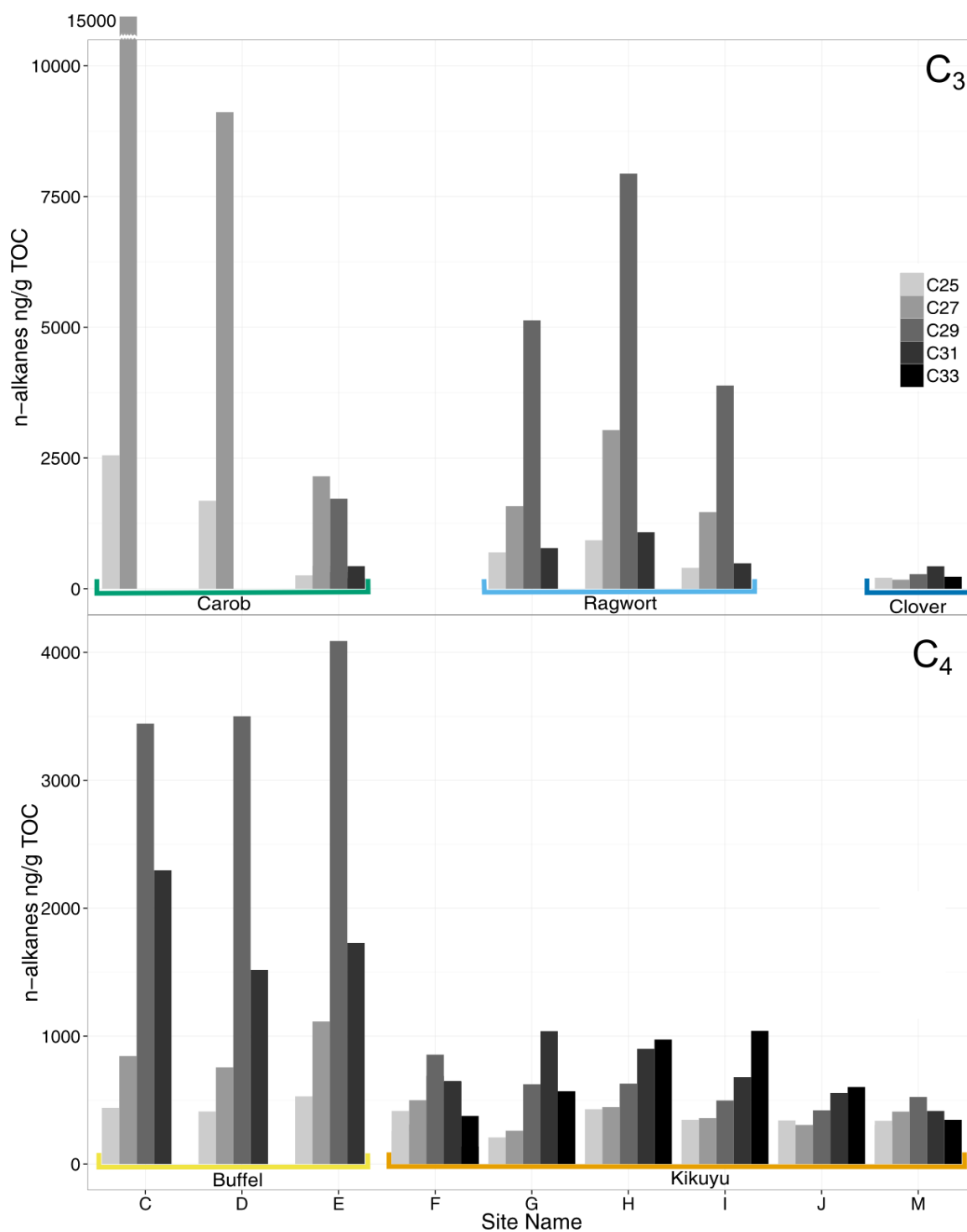


Figure 4. Quantities of *n*-alkanes per gram TOC per odd length alkanes C<sub>24</sub>-C<sub>33</sub>. Clover sample from site H resembled clover from site M, and is not shown. Buffel grass from site F resembled buffel grass from site E and is not shown. At sites I and M, data shown are averages of multiple specimens of the same species.

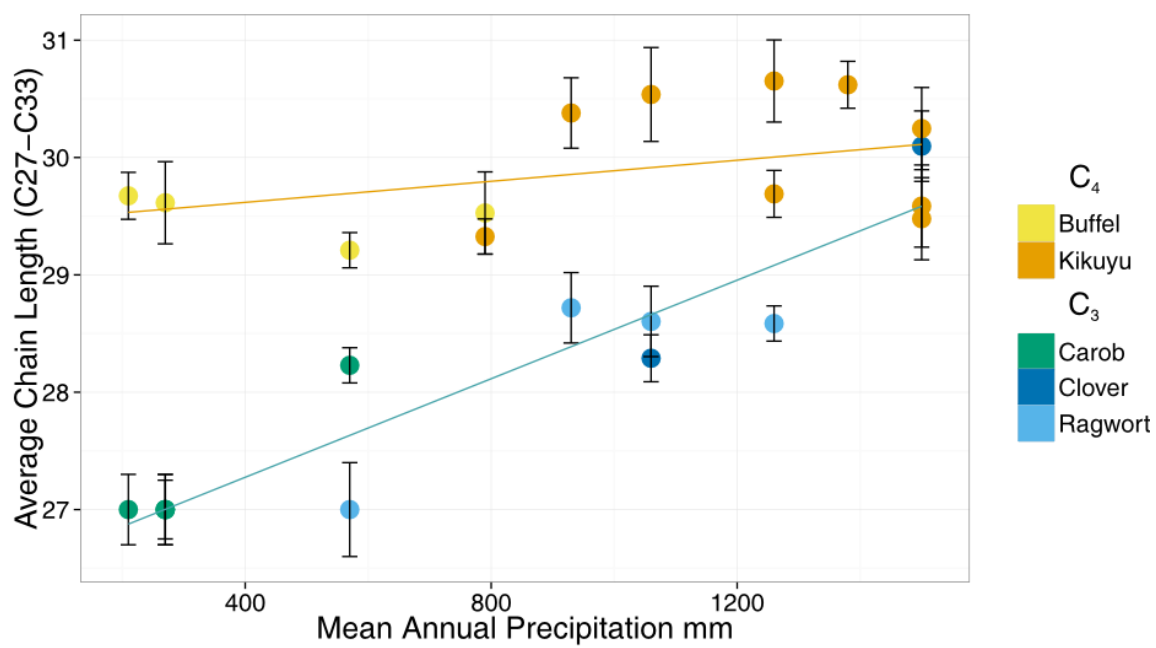


Figure 5. Average chain length calculated using C<sub>27</sub>-C<sub>33</sub> for each taxa as a function of precipitation. Linear regressions shown are significant at the p<0.05 level.

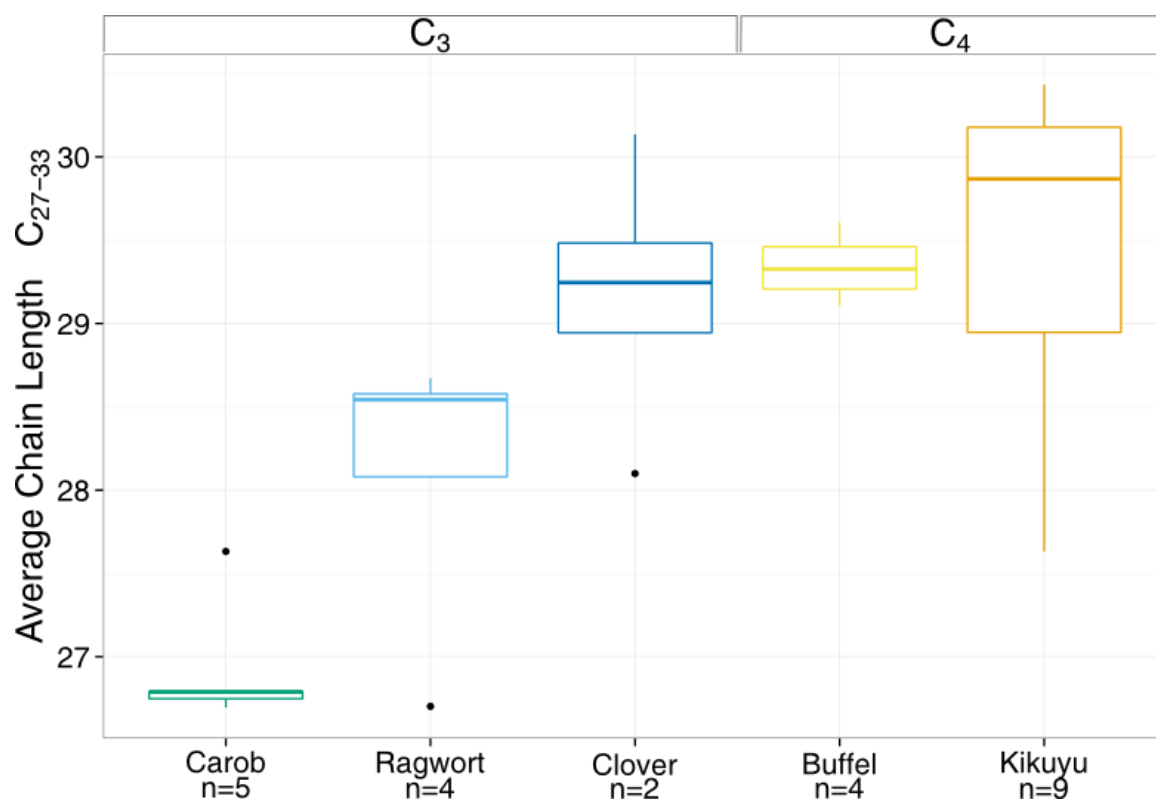


Figure 6. Boxplots of average chain length of individual species. Each box denotes the 25<sup>th</sup> to the 75<sup>th</sup> percentile the whiskers extend to the most extreme data point which is no more than 1.5 times the length of the box away from the box.

### Carbon isotopes of whole leaves

In C<sub>3</sub> plants,  $\delta^{13}\text{C}$  of leaf tissue decreased by 5‰ (24.6‰ to 30.2‰) from the driest to wettest sites (Table 4 and Figure 7). The isotopic range observed here is consistent with other published data for C<sub>3</sub> plants globally and in similar environments (Stewart et al., 1995; Chikaraishi and Naraoka, 2003; Prentice et al., 2011). Where more than one C<sub>3</sub> plant species was sampled at a site, they had similar  $\delta^{13}\text{C}$  values.

In contrast, C<sub>4</sub> grasses show relatively consistent carbon isotope values, around -13‰, at mid-range elevations. At the wettest sites (MAP >1060 mm MAP), Kikuyu grass displayed highly unusual signatures for C<sub>4</sub> plants, with leaf  $\delta^{13}\text{C}$  values 5‰ -15‰ lower than Kikuyu samples at drier sites. Leaf  $\delta^{13}\text{C}$  values for samples at the windward site (site M, 1500 mm MAP) resemble the carbon isotope values of C<sub>3</sub> plants. Linear regressions of  $\delta^{13}\text{C}_{\text{leaf}}$  and MAP were significant at the  $p < 0.05$  level in both C<sub>3</sub> and C<sub>4</sub> plants. Linear regressions of  $\delta^{13}\text{C}_{\text{leaf}}$  and MAP grouped by plant functional types were not significant (Table 6).

### Carbon isotopes of individual alkanes and $^{13}\epsilon_{\text{lipid}}$

The isotopic difference between lipids and leaves,  $^{13}\epsilon_{\text{lipid}}$ , remained relatively constant across the range of MAP sampled, especially for C<sub>27</sub> (Figure 7). Both  $\delta^{13}\text{C}$  and  $^{13}\epsilon_{\text{lipid}}$  varied more for C<sub>31</sub> than C<sub>27</sub>, and ranged from -29‰ to -35‰ and -1.2‰ to -8.6‰ respectively. Fractionation between the leaf and lipid carbon largely reflects the variability in the lipid isotope values, which varied more than 8‰ compared to leaf values that ranged only 5‰.  $^{13}\epsilon_{\text{lipid}}$  of C<sub>27</sub> was consistent across the range of MAP (-8.6‰ to -6.6‰) regardless of plant taxa or functional type (Figure 9).  $^{13}\epsilon_{\text{lipid}}$  of C<sub>29</sub> and C<sub>31</sub> average -6.2 ‰, and had no trend with MAP.

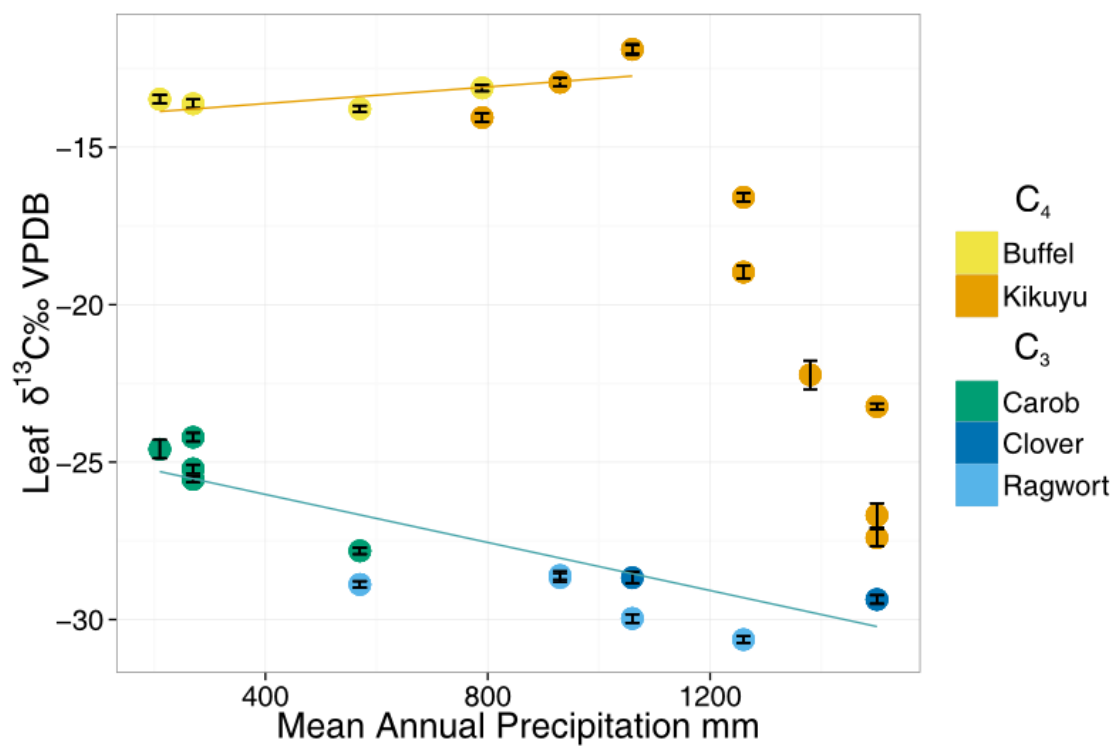


Figure 7.  $\delta^{13}\text{C}$  values for leaf tissue along the precipitation gradient. Linear regressions shown are significant at the  $p < 0.05$  level.



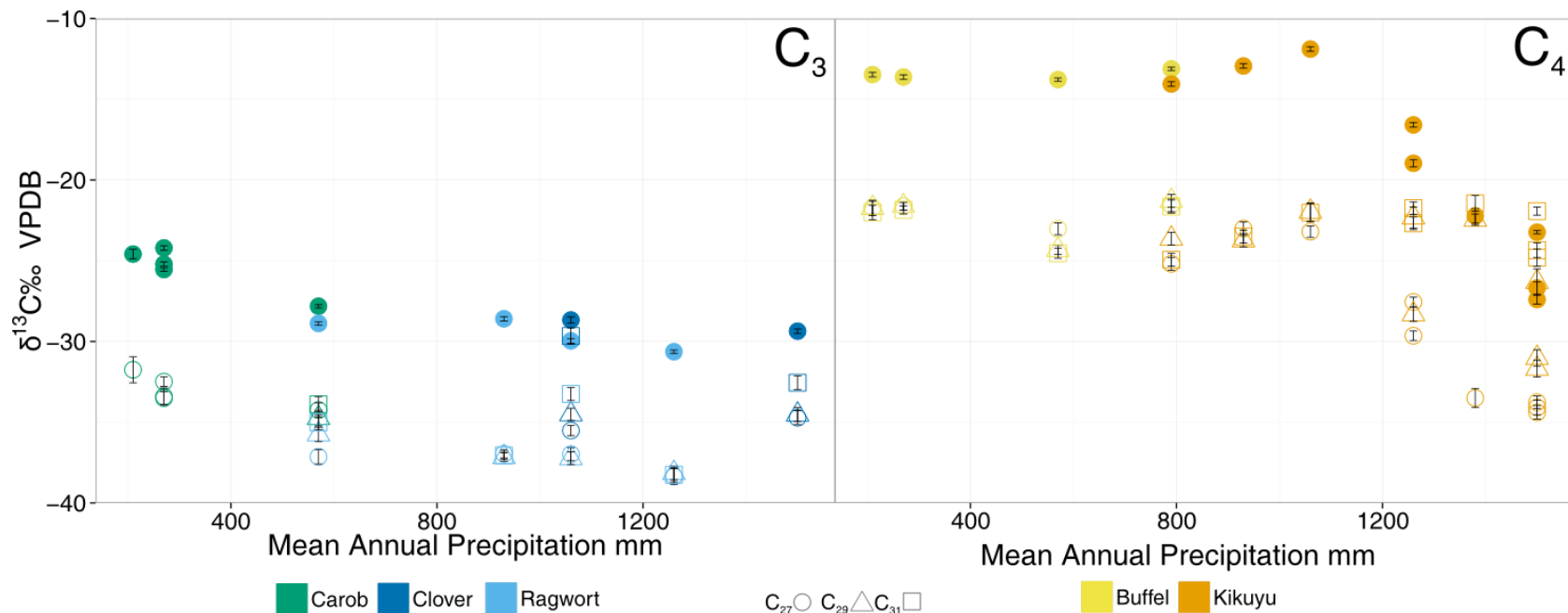


Figure 8.  $\delta^{13}C$  of leaves (filled circles), and lipids,  $C_{27}$  (open circles),  $C_{29}$  (open triangles), and  $C_{31}$  (open squares) along the precipitation gradient.

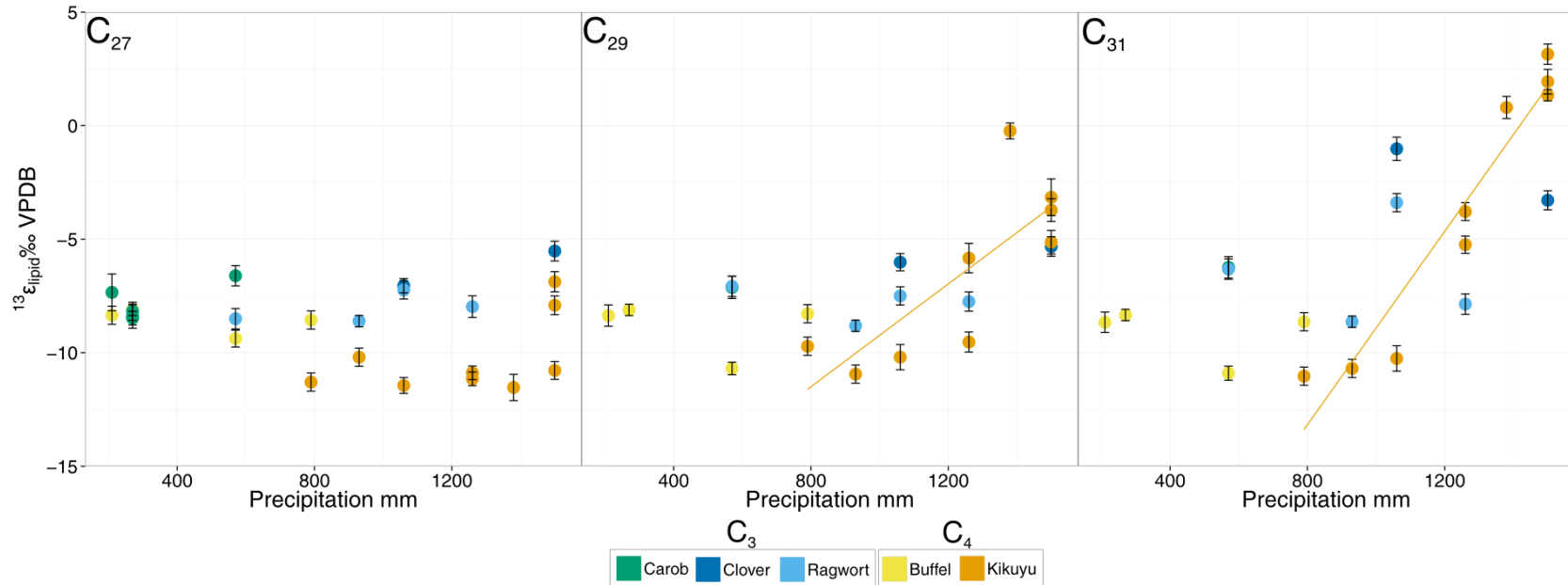


Figure 9. <sup>13</sup>ε<sub>lipid</sub> fractionation between leaf δ<sup>13</sup>C and lipid δ<sup>13</sup>C along the precipitation gradient. Note that in C<sub>29</sub>, <sup>13</sup>ε<sub>lipid</sub> of the tree sample from site E (570mm MAP) is the same as the value for the ragwort at that site. Linear regressions shown are significant a p<0.05 level.

In  $C_4$  grasses, alkanes  $C_{25}$  and  $C_{27}$  and shorter in length followed roughly the same trend as leaf carbon, namely,  $\delta^{13}C_{\text{lipid}}$  values were relatively constant up to 1060 mm MAP and decreased at sites above 1060 mm MAP. Kikuyu grass from wet sites show behavior uncharacteristic of  $C_4$  grasses.  $\delta^{13}C$  of  $C_{27}$  decreased sharply with increased MAP above 1060 mm (Figure 8).  $\delta^{13}C$  of  $C_{25}$  was even lower than  $C_{27}$ , and resembled lipids from  $C_3$  plants. Longer  $n$ -alkanes ( $C_{31}$  and  $C_{33}$ )  $\delta^{13}C$  values did not decrease, but continue the trend in  $\delta^{13}C_{\text{lipid}}$  established in sites C-H.

$^{13}\epsilon_{\text{lipid}}$  of  $C_{27}$  in the two grass species was distinct. Buffel grass averaged -8.6‰, where Kikuyu grass averaged -10.23‰ (-11.8‰ with site M excluded) (). Within each grass species, fractionation between the leaf and  $C_{27}$  did not change with MAP. For  $C_{29}$  or  $C_{31}$  at all sites, fractionation was more variable and buffel grass showed no trend, but Kikuyu grass showed statistically significant positive relationships with MAP (Table 7).

### Hydrogen isotopic composition of individual alkanes

Hydrogen isotope ratios in leaf waxes reflect the composition of source waters and physiological differences among plant functional types. (Chikaraishi and Naraoka, 2003; Magill et al., 2013b). Like these studies, at Kohala,  $C_3$  trees internally fractionate water isotopes less than  $C_3$  herbs or  $C_4$  grasses (Table 8, Figure 11).  $C_3$  trees were only sampled at three locations with similar climates. The tree at site E (674 mm MAP) was the only tree sampled with measureable quantities of alkanes longer than  $C_{27}$ . For this individual plant, longer alkane chains were more depleted in  $^2H$  than shorter alkanes (Figure 11).  $C_{27}$   $\delta^2H$  values ranged from -89‰ to -98‰, within the range of the sample taken at site E (570 mm MAP) for  $C_{29}$ .

For both grasses and herbs,  $C_{27}$  was slightly more depleted in  $^2H$  at higher MAP. In  $C_{27}$ , grass  $\delta^2H$  values were 20‰ lower, and  $^2\epsilon_{\text{lipid}}$  values were 11‰ lower than in  $C_3$  herbs. For  $C_{29}$  and

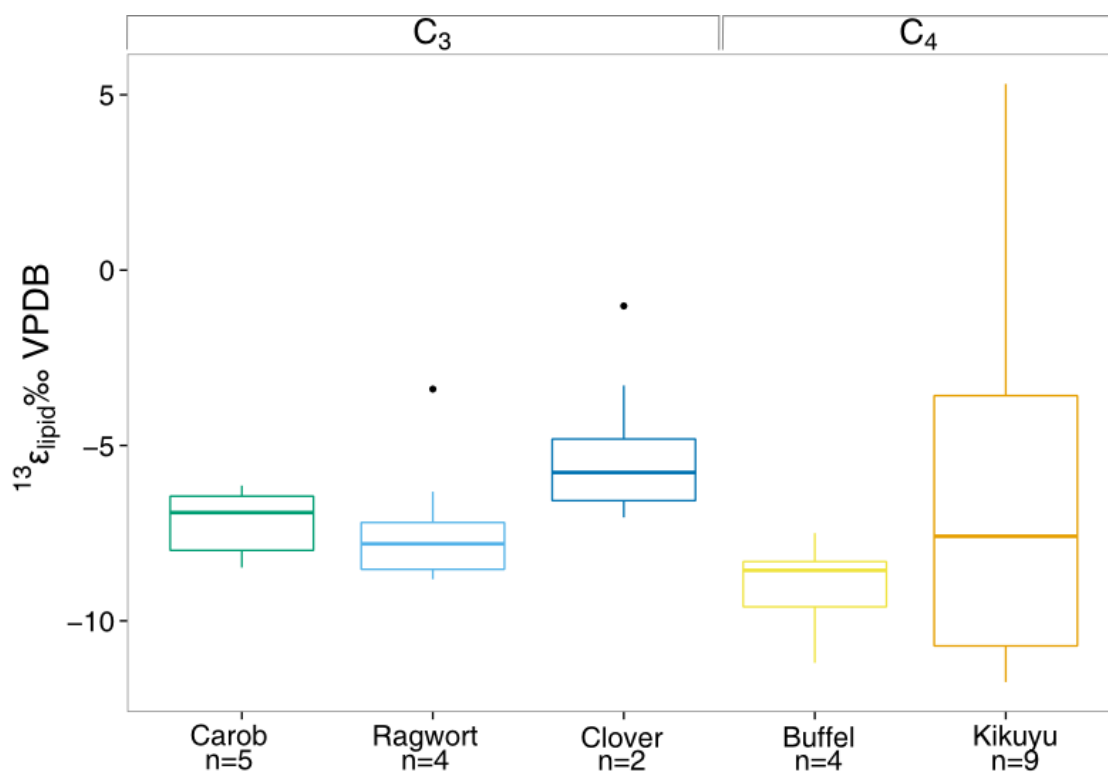


Figure 10. Boxplots of  $^{13}\epsilon_{\text{lipid}}$  of  $C_{27}$  for each sampled species combined from all sites. Each box denotes the 25<sup>th</sup> to the 75<sup>th</sup> percentile the whiskers extend to the most extreme data point which is no more than 1.5 times the length of the box away from the box.

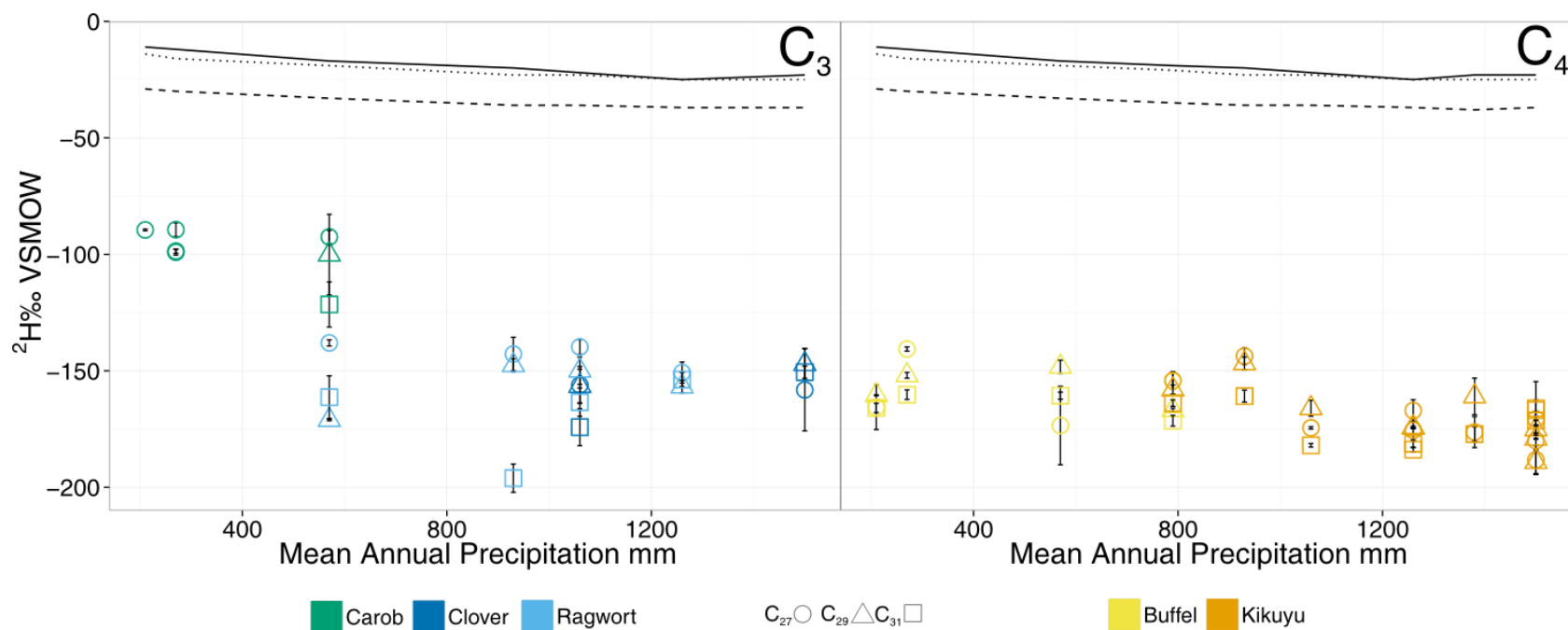


Figure 11.  $\delta^2\text{H}$  of lipids,  $C_{27}$  (open circles),  $C_{29}$  (open triangles), and  $C_{31}$  (open squares) and three models of  $\delta^2\text{H}$  of precipitation, Bowen and Revenaugh (2003) (solid line), Scholl et al (1995), trade winds area (dotted line), and Scholl et al. (1995) rain shadow area (dashed line).

$C_{31}$ ,  $\delta^2H$  differed little between  $C_4$  grasses and  $C_3$  herbs and collectively ranged -150‰ to -200‰ across the precipitation gradient. Only  $^2\epsilon_{lipid}$  of  $C_{29}$  in  $C_3$  herbs had a statistically significant positive relationship with MAP (Figure 12). Boxplots of  $C_{27}$   $^2\epsilon_{lipid}$  grouped by plant functional type (Figure 13) showed large differences between plant functional types. Figure 13 also shows  $^2\epsilon_{lipid}$  ranges identified by Magill et al., (2013). Kohala grasses averaged -147.6‰, corresponding to Magill's value of  $-146 \pm 8$ ‰ for  $C_4$  grasses. Kohala  $C_3$  herbs averaged -127.2‰ corresponding with  $-124 \pm 10$  from Magill et al (2013).  $C_3$  trees at Kohala averaged -78.2‰, much lower than Magill's value for  $C_3$  woody plants,  $-109 \pm 8$ ‰, but closer to the range reported for  $C_3$  shrubs,  $-87 \pm 4$ ‰.

### Carbon and Hydrogen Isotope Fractionation

Comparisons of  $^{13}\epsilon_{lipid}$  and  $^2\epsilon_{lipid}$  in  $C_{27}$  show  $C_3$  plants and buffel grasses clustering mostly within species (Figure 14). Kikuyu grass displays a similar range of  $^2\epsilon_{lipid}$  values as buffel grass, but has consistently lower  $^{13}\epsilon_{lipid}$  values, with the exception of two samples from the wettest site (site M). The increased variability in  $C_{29}$  and  $C_{31}$   $^2\epsilon_{lipid}$  mean there is less clustering by species in these plots. None of the linear regressions of  $^{13}\epsilon_{lipid}$  and  $^2\epsilon_{lipid}$  were significant at the  $p < 0.05$  level (Table 11).  $^{13}\epsilon_{lipid}$  and  $^2\epsilon_{lipid}$  of  $C_{29}$  Kohala data was plotted with data from Chikaraishi and Naraoka, 2003; Bi et al., 2005; Smith and Freeman, 2006; Krull et al., 2006, as presented by McInerney et al (2013) (Figure 15, Figure 16, and Appendix B, Table B1). The linear regression of  $^{13}\epsilon_{lipid}$  and  $^2\epsilon_{lipid}$  in all  $C_3$  plants was statistically significant (Table 12). When this same data was separated by plant functional type (Figure 16) the linear relationship between  $^{13}\epsilon_{lipid}$  and  $^2\epsilon_{lipid}$  in  $C_3$  plant mixed  $C_3$  grasses with  $C_3$  trees and herbs. None of the linear regressions of  $^{13}\epsilon_{lipid}$  and  $^2\epsilon_{lipid}$  in trees, herbs, and grasses, were significant at the  $p < 0.05$  level (Table 13).

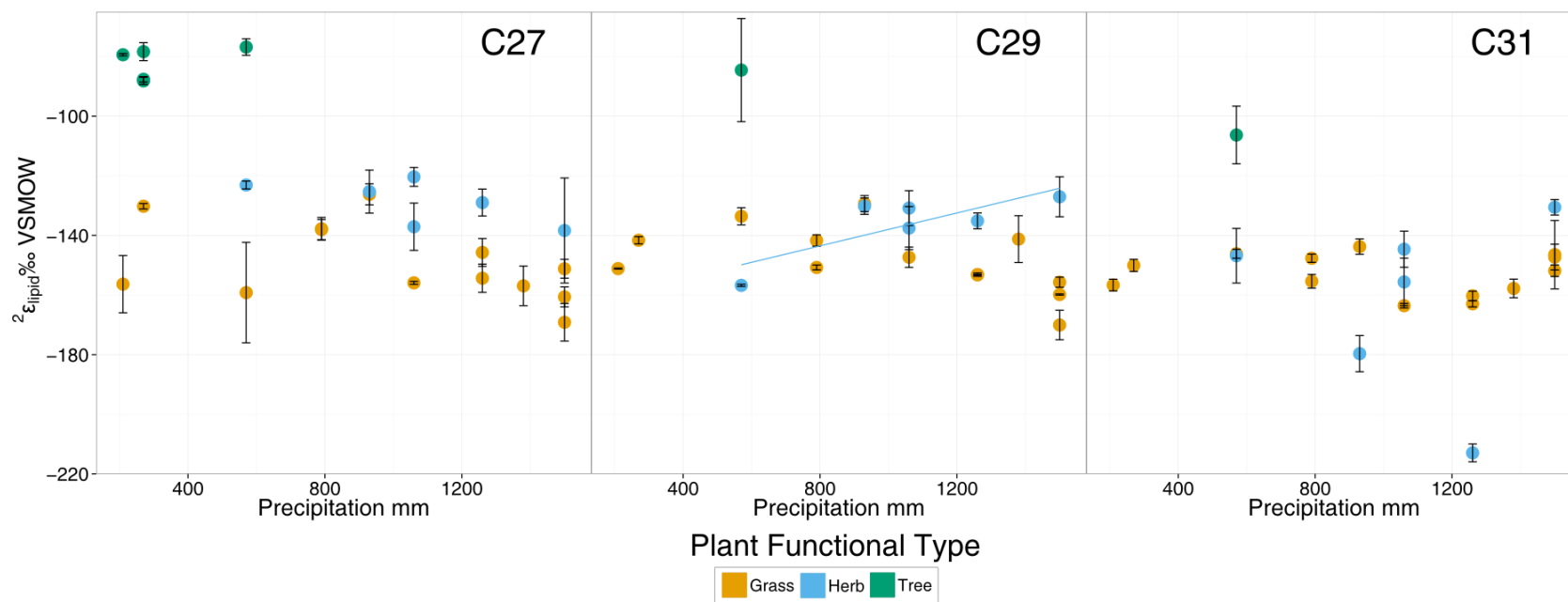


Figure 12.  ${}^2\epsilon_{\text{lipid}}$  fractionation between modeled  $\delta^2\text{H}$  of precipitation (from Bowen and Revenaugh 2003) and  $\delta^2\text{H}_{\text{lipid}}$  along the precipitation gradient. Linear regressions shown are significant at the  $p < 0.05$  level.

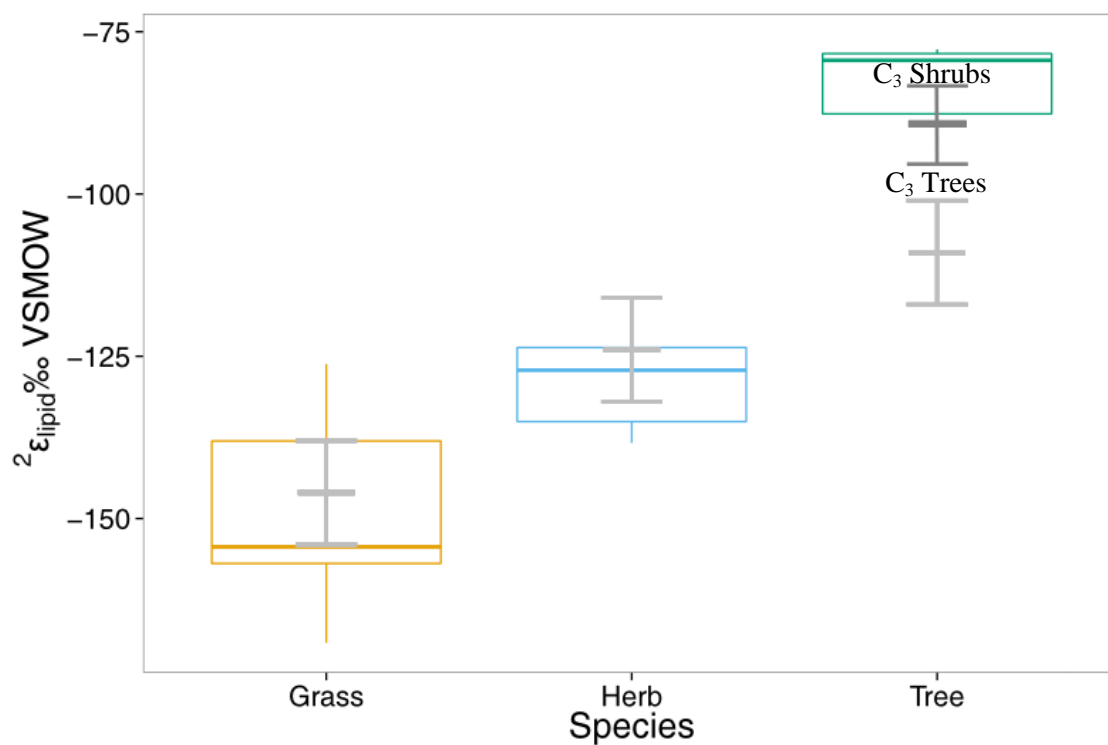


Figure 13. Boxplots of measured  $2\epsilon_{\text{lipid}}$  by PFT. Gray boxes represent  $2\epsilon_{\text{lipid}}$  ranges identified by Magill et al., (2013). C<sub>4</sub> grasses  $-146\text{‰} \pm 8\text{‰}$ , C<sub>3</sub> herbs:  $-124\text{‰} \pm 10\text{‰}$ ; C<sub>3</sub> woody plants:  $-109\text{‰} \pm 8\text{‰}$ ; and C<sub>3</sub> shrubs:  $-87\text{‰} \pm 4\text{‰}$ , dark grey. Each box denotes the 25<sup>th</sup> to the 75<sup>th</sup> percentile the whiskers extend to the most extreme data point which is no more than 1.5 times the length of the box away from the box.



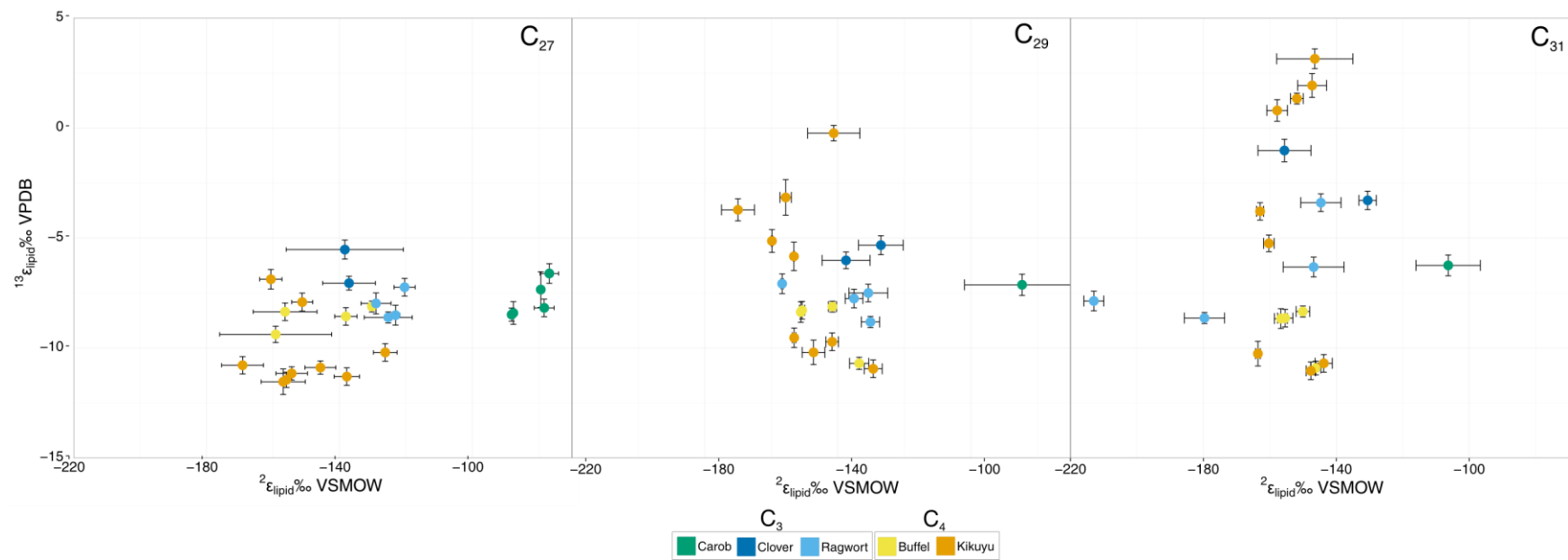


Figure 14.  $^{13}\epsilon_{\text{lipid}}$  and  $^2\epsilon_{\text{lipid}}$  of C<sub>27</sub>, C<sub>29</sub>, and C<sub>31</sub>

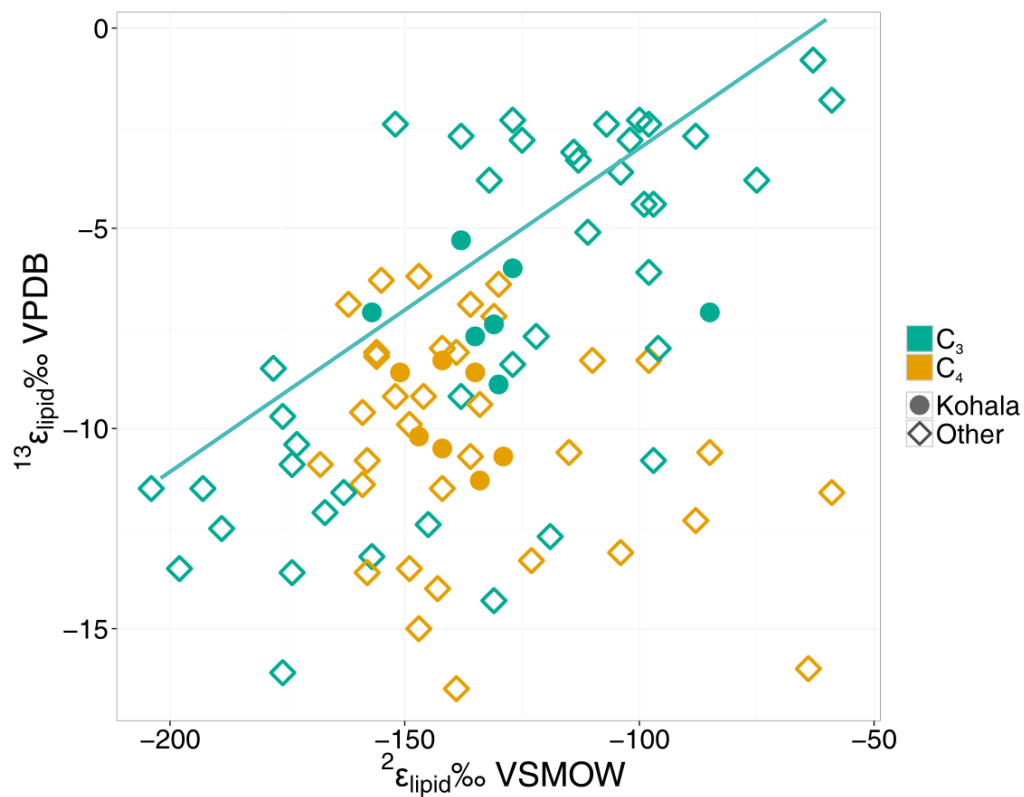


Figure 15,  $^2\epsilon_{\text{lipid}}$  and  $^{13}\epsilon_{\text{lipid}}$  of  $C_{29}$  for  $C_3$  and  $C_4$  plants from Chikaraishi and Naraoka, 2003; Bi et al., 2005; Smith and Freeman, 2006; Krull et al., 2006 and Kohala samples from this study. Linear regression of  $C_3$  plants is significant at the  $p < 0.05$  level.

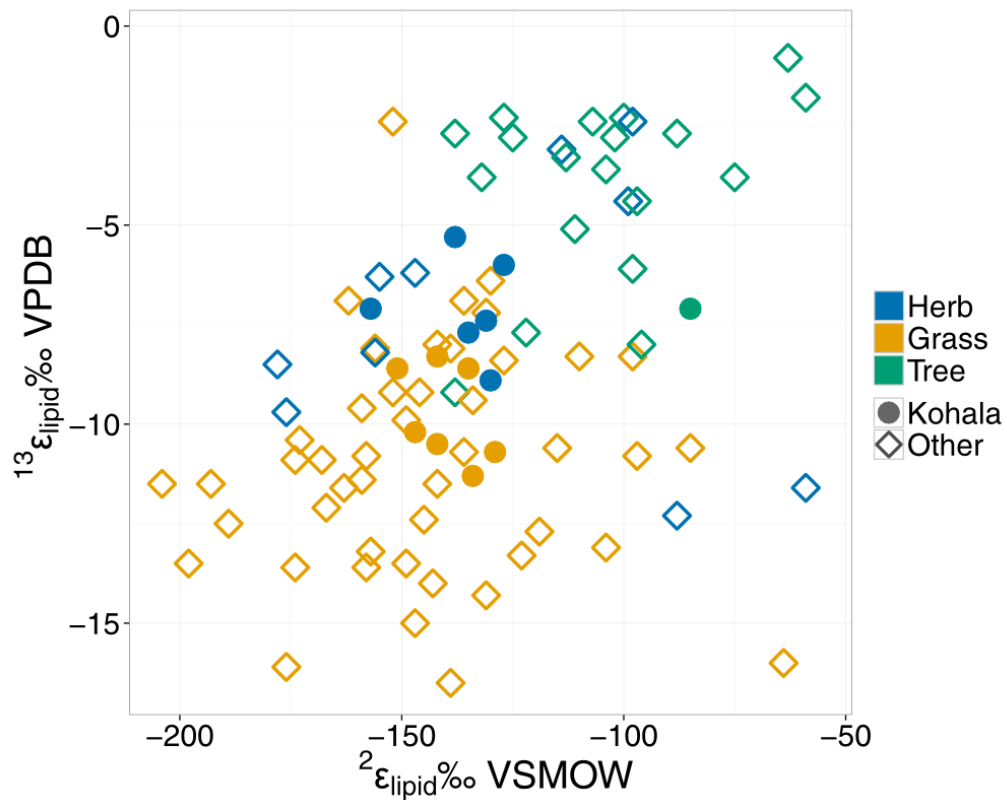


Figure 16.  $^2\epsilon_{\text{lipid}}$  and  $^{13}\epsilon_{\text{lipid}}$  of  $\text{C}_{29}$  for herbs, grasses and trees from Chikaraishi and Naraoka, 2003; Bi et al., 2005; Smith and Freeman, 2006; Krull et al., 2006 and Kohala samples from this study. None of the regressions were significant at the  $p < 0.05$  level.

## Discussion

### Alkane quantities and Average Chain Length

Taxonomic differences in leaf wax quantity were greater than changes in leaf waxes due to climate. Leaf waxes are usually assumed to protect leaves from desiccation (Gagosian, 1986; Gagosian and Peltzer, 1986; Sachse et al., 2006). On a coarse level, the data support this assumption. The C<sub>3</sub> tree sampled at the driest site (site C) had over 50% more total alkanes than the tree from the next, wetter site. In Carob trees and Kikuyu grass the quantity of *n*-alkanes increased slightly with aridity, but Ragwort, buffel grass, and clover were more variable (Figure 4). The variability in alkane production between plant types grown under the same condition indicates that taxonomy plays a larger role in the properties of *n*-alkanes than climate.

For the purposes of using *n*-alkanes as paleoclimate proxies it is more important to understand the biases in *n*-alkane production between plant types than to predict *n*-alkane quantity with climate. Like other studies, leaves from C<sub>3</sub> trees and herbs at Kohala contained an order of magnitude more alkanes than C<sub>4</sub> grasses (Diefendorf et al., 2011; Henderson et al., 2014). In addition, C<sub>3</sub> plants generally produce 20 times more biomass per area than C<sub>4</sub> plants. These two factors combine to underrepresent C<sub>4</sub> plants by as much as 200 times, relative to C<sub>3</sub> alkanes in the sedimentary record (Ehleringer, 1978; Still et al., 2003).

The differences in alkane quantity between plant types extend to the proportions of each alkane chain length. At Kohala, both C<sub>3</sub> and C<sub>4</sub> plants had longer ACL values at the wettest and coldest sites (Figure 5). This is counter to the general thinking that longer alkane chains help protect plants from drying out in hot environments (Gagosian, 1986; Gagosian and Peltzer, 1986; Sachse et al., 2006; Bush and Mcinerney, 2015). To test this, Sachse et al. (2006) sampled

deciduous trees from Finland to Italy, where precipitation ranged evenly from 450 mm to 1040 mm MAP, and temperatures clustered at 0-5 or 10-14 °C MAT (Appendix B, Figure B1). Sachse emphasized that ACL and temperature were positively correlated, but did not note that ACL was also strongly correlated with precipitation. Despite this oversight, data from Kohala and Sachse et al (2006) indicate ACL increases with rainfall for C<sub>3</sub> and C<sub>4</sub> plants in both temperate and tropical environments.

Given this finding, it is unlikely that longer alkane chains serve only to protect plants from drying out in hot environments. It is possible that cuticular alkanes protect plants from fungal attacks by contributing non-reactive molecules to the leaf surface (Bourdenx et al., 2011; Domínguez et al., 2011). In addition to physically protecting the leaf, the cuticle contains signaling and other bioactive structures which allow the plant to repel herbivores or produce more leaf waxes in response to external stimuli (Bourdenx et al., 2011). The composition of leaf wax alkanes is more dynamic than generally assumed by geochemists, although alkane isotope signatures are not dynamic after the leaf is formed (Tippie et al., 2013; Sachse et al., 2015). More work is necessary on the properties of leaf waxes including their antifungal qualities and taxonomic differences in alkane production.

The differences in ACL between plant functional types are greater than the precipitation trend (Figure 5). ACL increased by about 1.5 per 1000 mm MAP in C<sub>3</sub> plants. On average, ACL in trees was 2-4 lower than C<sub>3</sub> herbs. ACL of C<sub>4</sub> grasses increased by 0.5 across the transect, but was consistently higher than C<sub>3</sub> plants at the same site. Taxonomy had a greater effect on ACL than environmental moisture. As a result, the composition of the plant community would control the ecosystem level ACL value more than differences in temperature or climate.

To test this assumption, Carr et al., (2014) compared ACL from soils across South Africa to an aridity index. Overall, they observed longer ACL values at dry sites, and argued that this reflected the changing composition of plant communities across the sampled range. In the South

African sites, drier areas had a greater proportion of succulents and C<sub>4</sub> plants, both of which tend to produce longer alkane chains than C<sub>3</sub> plants. More recently, Bush and McInerney (2015) compared *n*-alkane properties in trees and some grasses at sites from Texas to Minnesota. They found ACL in plants and soils was most strongly correlated with mean summer temperature. The authors argue for a unified, taxa-wide increase in ACL with temperature, but data show notable taxonomic differences in ACL. The ACL of each taxa increased by about 1 from the coldest to warmest sites, and the taxa sampled were usually restricted to a small range of temperatures. The variation in ACL observed across the transect is larger than what is seen in any one taxa and is likely driven by the species composition of the site. Overall, temperature may correlate with ACL, but temperature is also driving plant community composition. At Kohala, there was an increase in ACL with MAP within species and PFT, but that difference was small compared to the differences between species and PFT. In geological samples, ACL will strongly reflect the plant composition of the ecosystem.

### **Carbon Isotopic Composition of C<sub>3</sub> Plant Leaves**

Leaf  $\delta^{13}\text{C}$  values for C<sub>3</sub> plants decreased with increased available moisture, similar to published and expected trends (Figure 2). The C<sub>3</sub> species sampled at Kohala showed a 4‰ to 6‰ depletion in carbon isotopes per 1000 mm increase in MAP (Figure 7 and Table 4), consistent with values for C<sub>3</sub> plants reported by Diefendorf et al. (2010), Krull et al. (2006), Ma et al. (2012), and Stewart et al. (1995), among others. These studies report data from diverse plant species and locations. The breadth of sampling in these studies may obscure trends between species, ecosystems, or plant functional types. The three species sampled at Kohala provide further evidence that the  $^{13}\text{C}$  signature of C<sub>3</sub> plants becomes more enriched in arid environments even within a single species.

Stewart et al. (1995) studied the  $\delta^{13}\text{C}$  of plant leaves across a climate gradient similar to Kohala. They averaged alkane properties from whole plant communities at tropical sites in northern Queensland. These sites ranged from 350 mm to 1700 mm MAP. The  $\delta^{13}\text{C}$  values from Queensland show a steeper slope with moisture than found in our limited sample, which likely reflects differences in plant community (Krull et al., 2006; Ma et al., 2012).

As expected,  $\delta^{13}\text{C}_{\text{lipid}}$  values of  $\text{C}_3$  plant waxes decreased with MAP with the same trend observed in bulk leaf tissues (Figure 8). Plants alter carbon allocation among lipids and other pools in response to the environment, which could alter the isotopic composition of each pool (Deniro and Epstein, 1977; Monson and Hayes, 1982). In this case, the apparent fractionation between carbon isotopes of leaves and lipids did not vary with MAP for  $\text{C}_3$  plants. For these plants, the biochemical partitioning of carbon within leaves was not influenced by climate. With this finding, paleoclimate studies of  $\text{C}_3$  dominated ecosystems can use modern estimates of  $^{13}\epsilon_{\text{lipid}}$  in similar species, without concern for the effects of local climate variation (Figure 9).

### **Carbon Isotopic Composition of $\text{C}_4$ Plant Leaves**

The  $\delta^{13}\text{C}$  of  $\text{C}_4$  leaves and lipids did not co-vary with MAP for samples collected at sites with less than 1060 mm annual rainfall (Figure 8). Enriched  $^{13}\text{C}$  values (-10‰ to -18‰ range) are considered diagnostic of plants that use  $\text{C}_4$  photosynthesis (Sage et al., 2011).  $\delta^{13}\text{C}$  values of leaves and lipids for  $\text{C}_4$  plants from dry sites averaged -13.2‰ and were well within this range (Troughton and Card, 1975; Farquhar et al., 1989; Cerling et al., 1997; Ehleringer et al., 1997). The  $\delta^{13}\text{C}$  value of  $\text{C}_4$  plants is not connected to environmental aridity because RuBisCo is isolated from the atmosphere in  $\text{C}_4$  plants (Figure 1) (Farquhar et al., 1989). Even between the two grass species,  $\delta^{13}\text{C}$  of  $\text{C}_4$  leaves and lipids were remarkably consistent from 250 mm to 1060 mm MAP.

The pattern in leaf  $\delta^{13}\text{C}$  values at the wettest sites was more difficult to explain. Counter to the accepted understanding of  $\text{C}_4$  photosynthesis,  $\delta^{13}\text{C}$  of  $\text{C}_4$  leaves gradually decreased as rainfall increased along the transect. There are three possible explanations: these plants were misidentified, depleted carbon was contributed by an external source, or these plants were not conducting standard  $\text{C}_4$  photosynthesis.

Kikuyu grass is distinctive, and not easily confused with any taxa of  $\text{C}_3$  grasses. It is commonly cited as a typical  $\text{C}_4$  grass, despite the fact that it is known to thrive in wetter and colder conditions than most  $\text{C}_4$  grasses (Buchmann et al., 1996; Wilen and Holt, 1996; Cusack et al., 2012; Muscolo et al., 2013). Misidentification is not likely.

It is also unlikely that fungal contamination contributed  $^{13}\text{C}$  depleted carbon to plant samples at wet sites. For example, in Douglas fir needles, epiphytic fungus only accounted for only -1 to -2‰ depletion in  $^{13}\text{C}$ , not the -5 to -15‰ observed here (El-hajj et al., 2004; Hobbie E et al., 2014). Additionally, none of the samples contained the even, short chain alkanes characteristic of fungi (Amelung and Brodowski, 2008).

Canopy structure can affect the  $\delta^{13}\text{C}$  of understory plants. Sites C-J were described as open-dry to mesic grassland with an occasional tree (Chadwick et al., 2007).  $\text{C}_4$  leaves and lipids from the driest of these sites (C-H) were predictably enriched in  $^{13}\text{C}$  compared to  $\text{C}_3$  plants from the same sites. The unexpected  $^{13}\text{C}$  depletion at the wettest sites (I, J, and M) coincides with a shift to a wet forest ecosystem (Chadwick et al., 2007). Kikuyu grass at these sites could have experienced changes in photosynthetic efficiency due to shading, and isotopic changes in the pool of available  $\text{CO}_2$ .

In closed canopy ecosystems, understory plants use previously respired  $\text{CO}_2$ , which is depleted in  $^{13}\text{C}$  relative to the atmosphere. In a dense forest, the  $\delta^{13}\text{C}$  of ambient  $\text{CO}_2$  in the understory can be lowered by 2 to 4‰, in turn both  $\text{C}_3$  and  $\text{C}_4$  leaves would become 2 - 4‰  $^{13}\text{C}$  depleted (Silveria et al., 1989; Buchmann et al., 1997; Pataki, 2003; Aranibar et al., 2006;



Graham, 2014). If canopy structure affects C<sub>4</sub> plants at this site, C<sub>3</sub> plants should be affected as well. The single C<sub>3</sub> clover plant sampled at site M was depleted in <sup>13</sup>C compared to samples from drier, open canopy sites, but not more than expected due to high moisture. This single data point, from a single plant, is not likely to represent the depleted <sup>13</sup>C of ambient CO<sub>2</sub> in the shaded understory. Without direct measurements of the understory δ<sup>13</sup>C of CO<sub>2</sub>, the strength of this effect is unknown.

In addition to changing understory CO<sub>2</sub>, forest cover shades the understory and can greatly reduce the efficiency of C<sub>4</sub> photosynthesis. C<sub>4</sub> grasses thrive in hot, high light environments. C<sub>4</sub> plants have an advantage over their C<sub>3</sub> counterparts because their spatial separation of photosynthesis and carbon assimilation limits photooxidation and water loss (Ehleringer et al., 1997). In low light environments, the advantage to C<sub>4</sub> plants is reduced compared to C<sub>3</sub> plants growing in the same conditions (Tieszen et al., 1979).

Additionally, in low light conditions, the incorporation of CO<sub>2</sub> into mesophyll cells can outpace the rate of carbon fixation in bundle sheath cells that causes a net leakage of carbon from mesophyll cells (Appendix B, Figure B2). In corn, leaky photosynthesis can result in a decrease of a 5-10 ‰ in the δ<sup>13</sup>C of leaves (Ubierna et al., 2013; Bellasio and Griffiths, 2014; Sage, 2014). This effect could account for part of the observed -15‰ depletion measured in carbon isotope values in Kikuyu grass from wet sites. Shade tolerant C<sub>4</sub> grasses like Kikuyu grass usually experience less leakage of CO<sub>2</sub> than other species, but leaky bundle sheath cells in shady conditions could still account for 5‰ to 10‰ of carbon isotope depletion. Neither leaky photosynthesis nor changes in the spacing of leaf veins have been documented in Kikuyu grass or its relatives, but either, or both, could explain the gradual decrease in δ<sup>13</sup>C values in Kikuyu grass along this climate gradient.

Although the findings at the wettest sites suggest a previously unknown flexibility in carbon assimilation by Kikuyu grass, it is probably not relevant for geochemical applications of

*n*-alkane proxies. C<sub>4</sub> grasses make up only a small portion of total biomass in wet and cold areas, like those measured at sites I, J, and M (Tieszen et al., 1979; Wilen and Holt, 1996; Muscolo et al., 2013). In the geologic record only a small portion of total organic carbon would be sourced from high altitude C<sub>4</sub> grasses like these, thus the geochemical implications of these sites is limited.

### **Fractionation between leaf and lipid carbon isotopes**

<sup>13</sup>ε<sub>lipid</sub> for C<sub>29</sub> averaged -7.3‰ for C<sub>3</sub> herbs and -7.1‰ for trees. This was lower than the -4 to -6 ‰ range commonly reported for temperate C<sub>3</sub> trees (from (Chikaraishi and Naraoka, 2003; Bi et al., 2005; Smith and Freeman, 2006; Krull et al., 2006; Diefendorf et al., 2011). At Kohala, <sup>13</sup>ε<sub>lipid</sub> values were indistinguishable between all C<sub>3</sub> taxa and buffel grass (Figure 9). <sup>13</sup>ε<sub>lipid</sub> values for Kikuyu grass were distinct from other taxa, indicating some level of taxonomic control on apparent fractionation in carbon isotopes (Figure 10). The difference between <sup>13</sup>ε<sub>lipid</sub> measured here, and values reported for other plants is most likely due to intrinsic taxonomic differences between the plants sampled, rather than local climate influencing carbon fractionation.

For buffel grass, <sup>13</sup>ε<sub>lipid</sub> values averaged -8.6 ‰ and were about 1‰ lower than those observed for C<sub>3</sub> plants in this study. With the exception of the wettest sites, <sup>13</sup>ε<sub>lipid</sub> values for Kikuyu lipids were ~2‰ lower than for buffel grass. Both are consistent with the larger fractionation factors observed in savannah grasses and the limited published data (Rommerskirchen, et al., 2006; McInerney et al., 2013; Magill et al., 2013b).

McInerney et al. (2013) aggregated carbon isotope measurements from published work, and compared <sup>13</sup>ε<sub>lipid</sub> to available moisture. They found <sup>13</sup>ε<sub>lipid</sub> values for both C<sub>3</sub> and C<sub>4</sub> plants became less negative with drier conditions, as measured by increased potential

evapotranspiration. The change was larger in C<sub>3</sub>, than in C<sub>4</sub> plants. Trends were similar in C<sub>29</sub> and C<sub>31</sub>, although there were greater variability in longer alkanes.

Unlike the transect at Kohala, which sampled the same five species grown in different conditions, McInerney et al. aggregated measurements from many species, locations, and growth environments (field grown, green house, botanical garden etc.). The combined data could have introduced patterns that reflect differences among species, plant functional type, or ecosystem structure, rather than trends that reflect individual plant responses to environment.

Other studies have also found  $^{13}\epsilon_{\text{lipid}}$  was insensitive to climate. Wei and Jia (2009) compared  $\delta^{13}\text{C}$  of soil organic matter (SOM) to  $\delta^{13}\text{C}$  of lipids from C<sub>4</sub> plants along a mountain transect. The values of both became more negative with altitude, but the fractionation between SOM and lipid carbon isotope values remained constant. Four species sampled at nine sites may not be globally representative, but this finding indicates that local climate does not change  $^{13}\epsilon_{\text{lipid}}$ . At the wet sites, I, J, and M, shorter alkanes (C<sub>25</sub> and C<sub>27</sub>) in Kikuyu leaves tracked  $\delta^{13}\text{C}_{\text{leaf}}$  values with a consistent fractionation factor, while the longer alkanes (C<sub>29</sub> and C<sub>31</sub>) were more enriched in  $^{13}\text{C}$ . The higher  $\delta^{13}\text{C}_{\text{lipid}}$  values resulted in overall smaller, and even positive,  $^{13}\epsilon_{\text{lipid}}$  values at the wettest site. What caused the discrepancy between fractionation factors for shorter and longer *n*-alkanes is not entirely clear. The divergence between carbon isotopes of shorter and longer alkanes only appears in Kikuyu grass. A flexible photosynthetic pathway might account for the discrepancy between  $\delta^{13}\text{C}$  lipid and leaf in these plants from wet sites. At drier study sites, longer lipids were more depleted in  $^{13}\text{C}$  than shorter lipids, following the pattern documented for other C<sub>3</sub> and C<sub>4</sub> plants (Chikaraishi et al., 2004; Bi et al., 2005). Even fewer studies exist on lipid fractionation in C<sub>3</sub>/C<sub>4</sub> intermediate and CAM plants. Two CAM plants studied by Chikaraishi et al. (2004) an increase in  $^{13}\text{C}$  depletion with increasing *n*-alcoholic acids chain length, similar to the pattern observed in the Kohala samples and Kikuyu grass.

### Hydrogen isotopes of individual alkanes and $^2\epsilon_{\text{lipid}}$

Hydrogen isotope fractionation observed between source water and leaf lipids ( $^2\epsilon_{\text{lipid}}$ ) is controlled by plant type. The photosynthetic pathway affects hydrogen fractionation due to leaf water loss through stomata, which differs in  $C_3$  and  $C_4$  plants (Smith and Freeman, 2006; Sachse et al., 2012). In geological samples, carbon isotope data for geological samples provide an estimate the ratio of  $C_3$  to  $C_4$  plants, or woody to non-woody vegetation in order to interpret the hydrogen isotopic values of lipids. Carbon isotopes are used to designate both plant functional type (PFT) and photosynthetic pathway.  $^2\epsilon_{\text{lipid}}$  values can be assigned based on PFT and  $C_3/C_4$  estimates and used to reconstruct the  $\delta^2\text{H}$  value of precipitation from the  $\delta^2\text{H}_{\text{lipid}}$  of geologic samples (Hren et al., 2010; Sachse et al., 2012; Magill et al., 2013b). This approach hinges on the assumption that estimates for  $^2\epsilon_{\text{lipid}}$  are well constrained across variable climates and that they do not change over time. Magill et al. (2013b) assembled published  $^2\epsilon_{\text{lipid}}$  values for different PFT, mostly from tropical rainforest environments, but including some savannah plants. It is uncertain how applicable these results are to the Kohala transect.

The  $\delta^2\text{H}$  and  $^2\epsilon_{\text{lipid}}$  values for  $C_{27}$  show consistent trends with MAP where the data for  $C_{29}$  and  $C_{31}$  are more variable (Figure 11 and Figure 12). Most paleoclimate studies that use *n*-alkanes focus on  $C_{29}$  and  $C_{31}$  (Sachse et al., 2006; Tipple and Pagani, 2010; McInerney et al., 2013; Magill et al., 2013b; Bush and McInerney, 2013) because  $C_{27}$  can be produced by some algae, lichen, and moss (Freeman and Pancost, 2014). The variations observed in  $C_{29}$  and  $C_{31}$  in samples may be due to the low concentrations of individual alkanes, and the analytical difficulty of obtaining a precise measurement on a small sample. For example, the single ragwort sample contained minute amounts of  $C_{31}$ , which caused more error in  $\delta^2\text{H}$  measurements (Figure 12). Where the measurements were robust, the isotope values of less abundant alkanes are isotopically variable. For  $C_3$  plants in regions with high water and plant-growth seasonality,  $\delta^2\text{H}_{\text{lipid}}$  is fixed

at the time of leaf flush (Tipple et al., 2013; Schwab et al., 2015). The climate conditions recorded in  $\delta^2\text{H}_{\text{lipid}}$  where there is little seasonal moisture differences are not known, but I suggest the lack of strong seasonal influences may reduce the variability of  $^2\epsilon_{\text{lipid}}$  overall.

$\text{C}_{27}$  values measured for  $\text{C}_3$  herbs and  $\text{C}_4$  grasses overlap with the  $^2\epsilon_{\text{lipid}}$  ranges identified by Magill et al., (2013). The mean of  $^2\epsilon_{\text{lipid}}$  values measured for  $\text{C}_3$  trees is 30‰ more enriched in  $^2\text{H}$  than the range identified by Magill et al., and the mean is closer to the values identified for  $\text{C}_3$  shrubs ( $-87 \pm 7\%$ ). Magill et al. used published values, from ecosystems that ranged from 183mm to more than 1200mm which should correspond to sites C, D and E, which only receive 210-570 mm MAP (Rommerskirchen, et al., 2006; Vogts et al., 2009). However, these trees may have a more shrub-like growth habit, or may grow in open conditions which may explain why these  $\text{C}_3$  trees have leaf lipid hydrogen isotope values that resemble data published for  $\text{C}_3$  shrubs (Rundel, 1980; Chadwick et al., 2007). These particular trees have a shrub-like stature and growth habitat. Further work is needed to identify independent means to differentiate between alkanes and their isotopic signals from shrubs and trees in geologic samples.

The Bowen and Revenaugh calculation method is used in other lipid studies, particularly when direct measurements of  $\delta^2\text{H}$  of precipitation are unavailable (McInerney et al., 2013; Magill et al., 2013b; Dupont et al., 2013; Leider et al., 2013). Although no direct measurements of  $\delta^2\text{H}$  of precipitation were made for my study on the Kohala peninsula, published measurements from the wet and dry areas near Hilo on Hawaii provide a point of comparison. Scholl et al. (1995 and 1996) found hydrogen isotopes gradients in precipitation differed considerably between rain shadow and trade wind-dominated areas. The Scholl et al. elevation-isotope relationships produced  $\delta^2\text{H}$  values for trade wind-dominated and rain shadow areas were 2‰ and 16‰ lower, respectively, than the Bowen and Revenaugh model. The differences between results from the three models (i.e., Bowen and Revenaugh, Scholl-leeward, and Scholl-windward) are relatively

small, especially when measured lipid  $\delta^2\text{H}$  values can range 50‰ for a single plant (Figure 11). The Scholl-leeward  $\delta^2\text{H}$  precipitation values yield  $^2\epsilon_{\text{lipid}}$  values that are higher by ~16‰ relative to those from the other two methods, and are also higher than the  $\epsilon_{\text{landscape}}$  ranges identified by Magill et al. (2013b). Based on similarities of the results to other studies (Magill et al., 2013b), I suggest the two other methods are the better choice to estimate rain isotope gradients, although direct observations are needed to properly establish lipid hydrogen isotope fractionation factors for the arid sites in Kohala.

### Carbon and hydrogen isotope fractionation

There is strong taxonomic control on the co-variance between  $^{13}\epsilon_{\text{lipid}}$  and  $^2\epsilon_{\text{lipid}}$   $\text{C}_{27}$  (Figure 14), shown by the tight clusters of data by species, excluding aberrant Kikuyu grass samples from wet sites. The relationship between  $^{13}\epsilon_{\text{lipid}}$  and  $^2\epsilon_{\text{lipid}}$  reflects photosynthetic and biosynthetic pathways, which vary by plant type and taxa and may not be equally sensitive to climate influences. In this data set,  $^{13}\epsilon_{\text{lipid}}$  and  $^2\epsilon_{\text{lipid}}$  do not co-vary, although they reveal groups by plant type, as previously reported by Chikaraishi et al. (2004) (Figure 15). McNerney et al. (2013) found that  $^{13}\epsilon_{\text{lipid}}$  and  $^2\epsilon_{\text{lipid}}$  co-vary in  $\text{C}_3$  plants, but not in  $\text{C}_4$  plants. When the Kohala data was compared with data from McNerney et al. (2013),  $^{13}\epsilon_{\text{lipid}}$  and  $^2\epsilon_{\text{lipid}}$  co-varied in all  $\text{C}_3$  plants (Figure 15 Table 12). Figure 16 shows this same data separated by plant functional type, which shows that the trend between  $^{13}\epsilon_{\text{lipid}}$  and  $^2\epsilon_{\text{lipid}}$  in  $\text{C}_3$  plants is due to the low  $^{13}\epsilon_{\text{lipid}}$  and  $^2\epsilon_{\text{lipid}}$  in  $\text{C}_3$  grasses. Within a plant functional type, there was no relationship between  $^{13}\epsilon_{\text{lipid}}$  and  $^2\epsilon_{\text{lipid}}$ . Based on the results from Kohala, I suggest trends in the McNerney et al., combined data set, are due to differences in sampled species that give the appearance of a  $^{13}\epsilon_{\text{lipid}}/{}^2\epsilon_{\text{lipid}}$  trend.

## Future work

The small set of samples from Kohala provides insights into how climate affects carbon and hydrogen isotopes in leaf wax alkanes. Although the study could be improved with samples from many more individual plants at each site, the data suggest the small sample sizes were nevertheless representative, especially for C<sub>4</sub> plants. Two Kikuyu grasses were sampled at site I, and three were sampled at site M. In each case, the multiple samples were similar to each other and intra-site variation is small. Multiple C<sub>3</sub> and C<sub>4</sub> representatives from each location would help resolve further the influences of differences between plant types relative to variations in plant responses to changes in climate. In general, the carbon isotope data for C<sub>3</sub> plants could be improved by sampling more C<sub>3</sub> species.

The enormous range in the carbon isotope values was unexpected for the Kikuyu grass. The dramatic decrease in <sup>13</sup>C content in Kikuyu leaves and lipids at the wet sites suggests previously reported flexibility in its photosynthetic strategies. Although it is unlikely that these grasses used CAM photosynthesis, samples could be tested for nighttime acid accumulation indicative of that photosynthetic pathway (Cernusak et al., 2013). It is more likely that these results are observed because wet sites were under partially closed canopy cover, and the low-growing grass and other understory plants were exposed to <sup>13</sup>C-depleted respired CO<sub>2</sub>. The δ<sup>13</sup>C of canopy air could be measured and used to calculate carbon isotope fractionation between atmospheric and leaf carbon (i.e. Δ<sup>13</sup>C<sub>leaf</sub>) (Buchmann et al., 1997). However, lower δ<sup>13</sup>C of air is probably insufficient to account for all of the observed carbon isotope depletion in C<sub>4</sub> grasses. I suggest Kikuyu grass underwent physiological changes along the strong moisture gradient that affected how it photosynthesizes carbon, and that these changes led to more C<sub>3</sub>-like carbon assimilation (Sage, personal communication). If so, evidence for this would be increased distance between veins on leaves of plants at wetter sites. Greenhouse experiments of Kikuyu grass in a

range of wet to dry, and sunny to shady treatments are needed to test the photosynthetic flexibility of this adaptive C<sub>4</sub> grass.

Direct measurements of  $\delta^2\text{H}$  of precipitation would improve calculations of  $^2\varepsilon_{\text{lipid}}$  values over the estimations presented here. Precipitation measurements could be combined with the earlier work by Scholl et al., (1995 and 1996) to help characterize water isotopes in rain shadows in the tropics. Additionally measurements of  $\delta^2\text{H}$  of soil, stem, and leaf water would allow the entire isotopic system to be characterized along the climate gradient.

The  $^2\varepsilon_{\text{lipid}}$  measurements from the species at Kohala are helpful to refine the  $\varepsilon_{\text{landscape}}$  ranges used by Magill et al. (2013b) but they still represent a small range of species in a single location. For the method proposed by Magill et al. to be robust, more examples of C<sub>4</sub> grasslands and mixed C<sub>3</sub>/C<sub>4</sub> ecosystems need to be studied.



## Conclusions

This study compared leaf wax *n*-alkanes properties across a precipitation gradient at the Kohala Peninsula of Hawaii. Overall, plant taxa had a stronger control on variability in alkane properties than climate. Although *n*-alkane quantity and ACL showed trends with precipitation, but differences between taxa were greater than changes due to climate.

In C<sub>3</sub> plants  $\delta^{13}\text{C}_{\text{leaf}}$  and  $\delta^{13}\text{C}_{\text{lipid}}$  decreased with increased MAP by 4 to 6‰ per 1000 mm increase in MAP. The apparent fractionation between leaf and lipid carbon isotopes ( $^{13}\epsilon_{\text{lipid}}$ ) was not affected by environmental moisture. These findings suggest that in C<sub>3</sub> dominated ecosystems,  $^{13}\epsilon_{\text{lipid}}$  is relatively free of the effects of local climate variation.

In C<sub>4</sub> grasses,  $\delta^{13}\text{C}_{\text{leaf}}$  and  $\delta^{13}\text{C}_{\text{lipid}}$  remained constant and enriched in <sup>13</sup>C for plants at sites with less than 1060 mm MAP. For this climate range,  $^{13}\epsilon_{\text{lipid}}$  was consistent and distinct for both grass species. For C<sub>4</sub> grasses at wet sites (MAP>1060mm), whole leaves and shorter *n*-alkanes (C<sub>25</sub> and C<sub>27</sub>) were unusually depleted in <sup>13</sup>C and their delta values resemble those of C<sub>3</sub> plants, while longer *n*-alkanes (C<sub>31</sub> and C<sub>33</sub>) remained enriched in <sup>13</sup>C and resemble lipids from C<sub>4</sub> plants from drier sites. The isotopic data suggest previously unrecognized flexibility in the photosynthetic pathway used by Kikuyu grass related to the influence of canopy cover at high rainfall sites. In addition to canopy cover depleting  $\delta^{13}\text{C}$  values of ambient CO<sub>2</sub>, I suspect Kikuyu grass converts to a more C<sub>3</sub> like form of photosynthesis to combat leakage of CO<sub>2</sub> from bundle sheath cells under shady conditions, which further decreases  $\delta^{13}\text{C}$  values. This combination of factors at wetter sites could account for the unusual  $\delta^{13}\text{C}$  values measured for Kikuyu grass leaves and lipids.

The hydrogen isotope fractionation between precipitation and leaf lipids was constant and specific to each plant functional type. Hydrogen isotopes of tropical C<sub>4</sub> grasses show no strong trends with aridity, and each plant functional type produces a distinct range of hydrogen isotope

values. The  $^2\epsilon_{\text{lipid}}$  values for C<sub>4</sub> grasses and C<sub>3</sub> herbs are similar to published values (Sachse et al., 2012; Magill et al. 2013b), although the  $^2\epsilon_{\text{lipid}}$  of C<sub>3</sub> trees at Kohala more closely correspond available data for C<sub>3</sub> shrubs consistent with the open and dry habitat of trees sampled in this study.

A combination of ACL and carbon isotopes of *n*-alkanes could be used to confirm and quantify the C<sub>4</sub> contribution to the *n*-alkane record. While we observed unexpected behavior of C<sub>4</sub> grasses in wet sites, these sites are not typical C<sub>4</sub> habitat and the contributions of C<sub>4</sub> derived alkanes to the geologic records from such sites is likely negligible.

## Appendix A: Tables

Table 1. Climate Variables . Site M is located on the windward and rainy side of the ridge.  $\delta^2\text{H}_{\text{precipitation}}$  modeled using Bowen and Revenaugh(2003) (BR), and Scholl et al (1995; 1996) for rain shadow (RS) and trade wind (TW) dominated areas .

Site	Elevation m	Distance from shore m	MAT C	MAP mm	Latitude	Longitude	$\delta^2\text{H}$ BR	$\delta^2\text{H}$ RS	$\delta^2\text{H}$ TW
C	256	2600	23	210	20.09166057	-155.8447297	-11	-29	-14
D	356	3311	22	270	20.08610576	-155.8291679	-12	-30	-26
E	674	6175	20	570	20.09804776	-155.8050031	-17	-33	-19
F	833	7343	19	790	20.09944243	-155.7927854	-19	-35	-21
G	922	8199	19	930	20.10471697	-155.7869535	-20	-36	-23
H	992	8752	18	1060	20.10803405	-155.7827209	-22	-36	-23
I	1090	9426	18	1260	20.10943833	-155.7761126	-23	-37	-25
J	1134	9965	18	1380	20.108446	-155.769747	-23	-38	-25
M	1104	13597	17	1500	20.10938579	-155.7268407	-25	-37	-25

Table 2. Linear regressions of total *n*-alkanes and mean annual precipitation. None of the regressions were significant at the 0.05 level.

	Total <i>n</i> -alkanes ng/g TOC			
	Slope	Intercept	R <sup>2</sup>	p
C4	-0.50	1010.05	0.32	0.089
C3	-3.24	9855.07	0.06	0.49
Herb	3.02	3998.60	0.04	0.75
Tree	-33.60	19248.60	0.54	0.16

Table 3. Quantities of individual *n*-alkanes in leaf samples.

Site	Species	PFT	Pathway	% TOC	<i>n</i> -alkanes ng/g TOC					Total
					C <sub>25</sub>	C <sub>27</sub>	C <sub>29</sub>	C <sub>31</sub>	C <sub>33</sub>	
C	Carob	Tree	C3	47	2552	15176				17728
D	Carob	Tree	C3	46	1104	2192				3296
D	Carob	Tree	C3	45	2032	7766				9798
D	Carob	Tree	C3	49	1683	9113				10795
E	Carob	Tree	C3	44	255	433	317	200		1205
E	Ragwort	Herb	C3	42	443	1720				2163
G	Ragwort	Herb	C3	41	695	1580	5133	777		8185
H	Clover	Herb	C3	41	290	906	1168	259		2623
H	Ragwort	Herb	C3	41	926	3034	7938	1081		12979
I	Ragwort	Herb	C3	43	400	1466	3884	486		6235
M	Clover	Herb	C3	42	210	172	279	428	228	1316
C	Buffel	Grass	C4	40	439	844	3443	2296	763	7786
D	Buffel	Grass	C4	43	411	756	3500	1518		6185
E	Buffel	Grass	C4	40	529	1115	4089	1728		7461
F	Buffel	Grass	C4	40	415	499	855	649	376	2794
F	Kikuyu	Grass	C4	43	329	366	935	728	255	2612
G	Kikuyu	Grass	C4	44	208	261	624	1039	569	2701
H	Kikuyu	Grass	C4	41	429	445	629	901	973	3376
I	Kikuyu	Grass	C4	40	346	359	497	679	1041	2922
I	Kikuyu	Grass	C4	40	311	347	461	540	719	2379
J	Kikuyu	Grass	C4	37	341	306	420	556	602	2225
M	Kikuyu	Grass	C4	41	338	410	524	415	346	2033
M	Kikuyu	Grass	C4	44	305	457	812	853	818	3246
M	Kikuyu	Grass	C4	37	296	335	458	364	311	1764

Table 4. Average chain length, leaf  $\delta^{13}\text{C}$ ,  $\delta^{13}\text{C}_{\text{lipid}}$ , and  $^{13}\text{C}_{\text{lipid}}$  of leaf wax *n*-alkanes. ACL was calculated using  $\text{C}_{27}$ ,  $\text{C}_{29}$ ,  $\text{C}_{31}$ , and  $\text{C}_{33}$ .

Site	Species	PFT	Pathway	ACL	Leaf	$\delta^{13}\text{C}_{\text{lipid}}$ ‰ VPDB				$^{13}\text{C}_{\text{lipid}}$ ‰ VPDB			
						$\text{C}_{27}$	$\text{C}_{29}$	$\text{C}_{31}$	$\text{C}_{33}$	$\text{C}_{27}$	$\text{C}_{29}$	$\text{C}_{31}$	$\text{C}_{33}$
C	Carob	Tree	C3	26.8	-24.6±0.8	-31.8±0.8				-7.3±0.8			
D	Carob	Tree	C3	26.7	-24.2±0.4	-32.5±0.3				-8.5±0.3			
D	Carob	Tree	C3	26.7	-25.2±1.3	-33.4±0.5				-8.4±0.5			
D	Carob	Tree	C3	26.8	-25.5±1	-33.5±0.4				-8.2±0.4			
E	Carob	Tree	C3	29.6	-27.8±0.4	-34.2±0.4	-34.7±0.5	-33.9±0.5		-6.6±0.4	-7.1±0.5	-6.2±0.5	
E	Ragwort	Herb	C3	29	-28.9±1.1	-37.1±0.5	-35.8±0.5	-35±0.5		-8.5±0.5	-7.1±0.5	-6.3±0.5	
G	Ragwort	Herb	C3	29.1	-28.6±0.1	-37±0.3	-37.2±0.3			-8.6±0.3	-8.8±0.3	-8.6±0.3	
H	Ragwort	Herb	C3	29.1	-30±2.2	-37±0.4	-37.2±0.4	-33.3±0.4		-7.2±0.4	-7.5±0.4	-3.4±0.4	
I	Ragwort	Herb	C3	29.1	-30.6±0.2	-38.4±0.5	-38.1±0.4			-8±0.5	-7.7±0.4	-7.9±0.4	
H	Clover	Herb	C3	29.2	-28.7±2.7	-35.5±0.3	-34.5±0.4	-29.7±0.5		-7±0.3	-6±0.4	-1±0.5	
M	Clover	Herb	C3	30.1	-29.4±1.5	-34.7±0.4	-34.5±0.4	-32.6±0.4		-5.5±0.4	-5.3±0.4	-3.3±0.4	
C	Buffel	Grass	C4	29.8	-13.5±0.2	-21.7±0.4	-21.7±0.5	-22±0.5		-8.4±0.4	-8.4±0.5	-8.7±0.5	
D	Buffel	Grass	C4	29.5	-13.6±0.1	-21.6±0.3	-21.6±0.3	-21.8±0.3		-8.1±0.3	-8.1±0.3	-8.3±0.3	
E	Buffel	Grass	C4	30	-14.1±1.5	-23±0.4	-24.3±0.3	-24.5±0.3	-24.8±0.9	-9.1±0.4	-10.4±0.3	-10.6±0.3	-10.9±0.9
F	Buffel	Grass	C4	29.9	-13.1±0.7	-21.6±0.4	-21.3±0.4	-21.6±0.4	-22.8±0.4	-8.6±0.4	-8.3±0.4	-8.6±0.4	-9.8±0.4
F	Kikuyu	Grass	C4	29.5	-13.8±0.8	-25.2±0.4	-23.6±0.4	-24.9±0.4		-11.6±0.4	-10±0.4	-11.3±0.4	
G	Kikuyu	Grass	C4	30.8	-12.9±0.3	-23±0.4	-23.7±0.4	-23.5±0.4	-23.2±0.4	-10.2±0.4	-10.9±0.4	-10.7±0.4	-10.4±0.4
H	Kikuyu	Grass	C4	31.2	-11.9±0.6	-23.2±0.4	-22±0.6	-22±0.6	-22.7±0.6	-11.4±0.4	-10.2±0.6	-10.3±0.6	-10.9±0.6
I	Kikuyu	Grass	C4	31.4	-16.6±2.7	-27.6±0.3	-22.3±0.6	-21.7±0.4	-22.3±0.4	-11.2±0.3	-5.8±0.6	-5.2±0.4	-5.8±0.4
I	Kikuyu	Grass	C4	31.1	-19±3.4	-29.6±0.3	-28.3±0.4	-22.7±0.4	-22.7±0.4	-10.9±0.3	-9.5±0.4	-3.8±0.4	-3.8±0.4
J	Kikuyu	Grass	C4	31.1	-22.2±6.3	-33.5±0.6	-22.5±0.4	-21.4±0.5	-22.2±0.5	-11.5±0.6	-0.2±0.4	0.8±0.5	0±0.5
M	Kikuyu	Grass	C4	30.3	-27.4±5.2	-34.1±0.4	-31±0.5	-24.3±0.4	-22.2±0.5	-6.9±0.4	-3.7±0.5	3.1±0.4	5.3±0.5
M	Kikuyu	Grass	C4	30.8	-23.2±5.7	-33.8±0.4	-26.3±0.8	-21.9±0.3	-21±0.4	-10.8±0.4	-3.2±0.8	1.3±0.3	2.3±0.4
M	Kikuyu	Grass	C4	30.2	-26.7±5.6	-34.4±0.4	-31.7±0.5	-24.8±0.5	-22±0.4	-7.9±0.4	-5.1±0.5	1.9±0.5	4.8±0.4

Table 5. Linear regression of ACL and mean annual precipitation. P-values in bold italics are significant at the 0.05 level.

	Average Chain Length			
	Slope	Intercept	R <sup>2</sup>	p
C <sub>3</sub>	0.002	26.58	0.81	<b><i>0.0004</i></b>
C <sub>4</sub>	0.001	29.16	0.42	<b><i>0.043</i></b>

Table 6. Linear regression of  $\delta^{13}\text{C}_{\text{leaf}}$  and mean annual precipitation. P-values in bold italics are significant at the 0.05 level.

	Leaf $\delta^{13}\text{C}$			
	Slope	Intercept	R <sup>2</sup>	p
Grass all sites	-0.010	-7.967	0.61	<b><i>1.55x10<sup>-14</sup></i></b>
Grass not I, J, or M	-0.001	-14.14	0.35	<b><i>1.44x10<sup>-4</sup></i></b>
Herbs	-0.001	-27.59	0.01	0.62
Trees	-0.009	-22.55	0.88	<b><i>6.22x10<sup>-12</sup></i></b>
C <sub>3</sub>	-0.004	-23.23	0.27	<b><i>1.04x10<sup>-4</sup></i></b>



Table 7. Linear regression of  $^{13}\epsilon_{\text{lipid}}$  values and mean annual precipitation. P-values in bold italics are significant at the 0.05 level.

	$C_{27}$				$C_{29}$				$C_{31}$			
	Slope	Intercept	$R^2$	p	Slope	Intercept	$R^2$	p	Slope	Intercept	$R^2$	p
$C_3$	0.001	-8.459	0.2280	0.089	0.001	-8.33	0.140	0.404	0.0002	-7.94	0.12	0.448
Carob	0.004	-9.081	0.511	0.175	NA	NA	NA	NA	NA	NA	NA	NA
Clover	0.003	-10.72	NA	NA	0.001	-7.678	NA	NA	-0.005	4.43	NA	NA
Ragwort	0.001	-9.208	0.298	0.454	-0.001	-7.007	0.10	0.681	-0.0004	-6.154	0.00	0.94
$C_4$	-0.001	-8.936	0.0520	0.462	0.004	-11.73	0.38	<b><i>0.025</i></b>	0.009	-14.81	0.60	<b><i>0.001</i></b>
Buffel	-0.001	-8.122	0.261	0.499	-0.001	-8.287	0.08	0.722	-0.001	-8.505	0.10	0.689
Kikuyu	0.003	-14.28	0.261	0.160	0.011	-20.54	0.63	<b><i>0.011</i></b>	0.021	-30.21	0.92	<b><i><math>3.8 \times 10^{-5}</math></i></b>

Table 8.  $\delta^2\text{H}\%$  VSMOW of precipitation modeled after Bowen and Revenaugh (2003), measured  $\delta^2\text{H}_{\text{lipid}}$ , and  $^2\epsilon_{\text{lipid}}$  of leaf wax *n*-alkanes.

Site	Species	PFT	Pathway	$\delta^2\text{H}$ Precipitation	$\delta^2\text{H}_{\text{lipid}} \%$ VSMOW				$^2\epsilon_{\text{lipid}} \%$ VSMOW				
					C <sub>27</sub>	C <sub>29</sub>	C <sub>31</sub>	C <sub>33</sub>	C <sub>27</sub>	C <sub>29</sub>	C <sub>31</sub>	C <sub>33</sub>	
C	Carob	Tree	C3	-11	-90±2					-79±1			
D	Carob	Tree	C3	-12	-99±3					-88±1			
D	Carob	Tree	C3	-12	-99±3					-88±2			
D	Carob	Tree	C3	-12	-89±3					-78±3			
E	Carob	Tree	C3	-17	-93±3	-100±17	-122±10			-77±3	-85±17	-106±10	
E	Ragwort	Herb	C3	-17	-138±3	-171±2	-161±9			-123±1	-157±1	-147±9	
G	Ragwort	Herb	C3	-20	-143±7	-148±3	-196±6			-125±7	-130±3	-180±6	
H	Ragwort	Herb	C3	-22	-140±3	-150±6	-163±6			-120±3	-131±6	-145±6	
I	Ragwort	Herb	C3	-25	-151±5	-157±3	-154±3			-129±5	-135±3	-213±3	
H	Clover	Herb	C3	-22	-156±8	-157±7	-174±8			-137±8	-138±7	-156±8	
M	Clover	Herb	C3	-23	-158±18	-147±7	-151±3	-169±3		-138±18	-127±7	-131±3	-150±3
C	Buffel	Grass	C4	-11	-166±10	-160±2	-166±4			-156±10	-151±1	-157±2	
D	Buffel	Grass	C4	-12	-141±3	-152±3	-160±2			-130±2	-142±1	-150±2	
E	Buffel	Grass	C4	-17	-173±17	-148±3	-161±4	-203±24		-159±17	-134±3	-146±4	-190±24
F	Buffel	Grass	C4	-19	-154±3	-167±3	-171±2	-176±2		-138±3	-151±2	-155±2	-160±1
F	Kikuyu	Grass	C4	-19	-154±4	-158±4	-164±3			-138±4	-142±4	-148±3	
G	Kikuyu	Grass	C4	-20	-144±4	-147±3	-161±3	-168±2		-126±4	-129±3	-144±3	-151±2
H	Kikuyu	Grass	C4	-22	-174±2	-166±3	-182±3	-184±2		-156±1	-147±3	-164±2	-165±1
I	Kikuyu	Grass	C4	-25	-176±5	-174±2	-181±4	-183±3		-154±5	-153±0	-160±2	-162±1
I	Kikuyu	Grass	C4	-25	-167±5	-174±3	-184±3	-185±4		-146±5	-153±2	-163±1	-164±4
J	Kikuyu	Grass	C4	-23	-176±7	-161±8	-177±3	-171±6		-157±7	-141±8	-158±3	-151±6
M	Kikuyu	Grass	C4	-23	-180±3	-189±5	-166±11	-165±11		-161±3	-170±5	-146±11	-145±11
M	Kikuyu	Grass	C4	-23	-188±6	-175±4	-171±4	-167±3		-169±6	-156±2	-152±2	-147±1
M	Kikuyu	Grass	C4	-23	-171±3	-179±2	-167±4	-169±3		-151±3	-160±1	-147±4	-149±1



Table 10. Linear regressions of  $\delta^{13}\text{C}$  and  $^2\varepsilon_{\text{lipid}}$ . P-values in bold italics are significant at the 0.05 level.

	$\text{C}_{27}$				$\text{C}_{29}$				$\text{C}_{31}$			
	Slope	Intercept	$\text{R}^2$	p	Slope	Intercept	$\text{R}^2$	p	Slope	Intercept	$\text{R}^2$	p
$\text{C}_3$	0.064	-28.06	0.57	<b><i>0.01</i></b>	0.019	-33.5	0.08	0.53	0.051	-26.41	0.37	0.15
$\text{C}_4$	0.226	6.745	0.30	<b><i>0.05</i></b>	0.201	5.184	0.38	<b><i>0.02</i></b>	0.0139	-44.14	0.49	<b><i>0.01</i></b>

Table 11. Linear regressions of  $^{13}\epsilon_{\text{lipid}}$  and  $^2\epsilon_{\text{lipid}}$ . P-values in bold italics are significant at the 0.05 level.

	$C_{27}$				$C_{29}$				$C_{31}$			
	Slope	Intercept	$R^2$	p	Slope	Intercept	$R^2$	p	Slope	Intercept	$R^2$	p
$C_3$	-0.009	-8.895	0.05	0.49	-0.0003	-7.124	$3.3 \times 10^{-5}$	0.99	0.034	-0.001	0.19	0.34
$C_4$	0.008	-8.576	0.003	0.84	-0.151	-29.70	0.25	0.08	0.007	-4.208	$9.6 \times 10^{-5}$	0.97

Table 12. Linear regressions of  $C_{29}^{2}\epsilon_{lipid}$  and  $^{13}\epsilon_{lipid}$  for  $C_3$  and  $C_4$  plants from (Chikaraishi and Naraoka, 2003; Smith and Freeman, 2006; Sachse et al., 2006; Rommerskirchen, et al., 2006; Krull et al., 2006; Pedentchouk et al., 2008; Feakins and Sessions, 2010; Diefendorf et al., 2011) Bi et al. (2005); Hou et al. (2007); Liu & Yang (2008); Liu & Yang (2008), Liu et al. (2006); Liu et al. (2006); Sachse et al. (2009); Sessions (2006); Yang and Huang (2003); Kahmen et al. (2013); Duan & He (2011); Diefendorf et al (2011); Rommerskirchen et al. (2007); Rommerskirchen et al. (2008); Rommerskirchen et al. (2009). P-values in bold italics are significant at the  $p < 0.05$  level.

	Total <i>n</i> -alkanes ng/g TOC			
	Slope	Intercept	R <sup>2</sup>	p
C4	-2.252	-156.83	0.04815	0.1856
C3	5.989	-87.485	0.4725	<b><i>4.1e-8</i></b>

Table 13. Linear regressions of  $C_{29}^{2}\epsilon_{lipid}$  and  $^{13}\epsilon_{lipid}$  for herbs, grasses and trees from (Chikaraishi and Naraoka, 2003; Smith and Freeman, 2006; Sachse et al., 2006; Rommerskirchen, et al., 2006; Krull et al., 2006; Pedentchouk et al., 2008; Feakins and Sessions, 2010; Diefendorf et al., 2011) Bi et al. (2005); Hou et al. (2007); Liu & Yang (2008); Liu & Yang (2008), Liu et al. (2006); Liu et al. (2006); Sachse et al. (2009); Sessions (2006); Yang and Huang (2003); Kahmen et al. (2013); Duan & He (2011); Diefendorf et al (2011); Rommerskirchen et al. (2007); Rommerskirchen et al. (2008); Rommerskirchen et al. (2009) None of the regressions were significant at the  $p < 0.05$  level.

	Total <i>n</i> -alkanes ng/g TOC			
	Slope	Intercept	R <sup>2</sup>	p
Grass	0.6164	-137.7309	0.003868	0.6582
Herb	-0.6091	-134.8818	0.002681	0.8501
Tree	2.795	-92.441	0.08096	0.224

## Appendix B: Supplemental Figures and Data

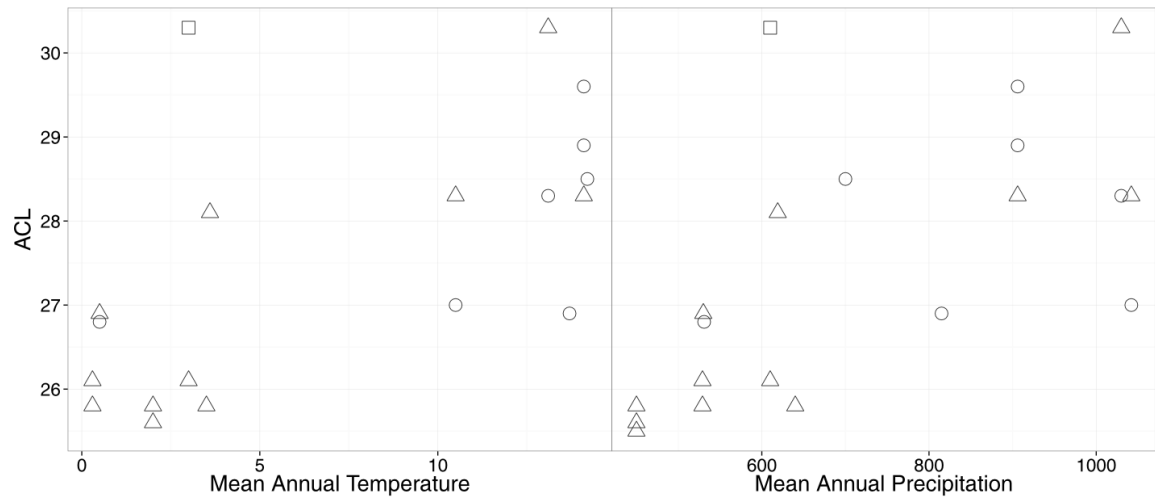


Figure B1. ACL and mean annual temperature and precipitation from Sachse et al (2006?).

Deciduous trees were sampled in a transect from Finland to Italy. ACL increases with MAT and MAP for Myrtaceae (squares), Betulaceae (circles) and Fagaceae (triangles).



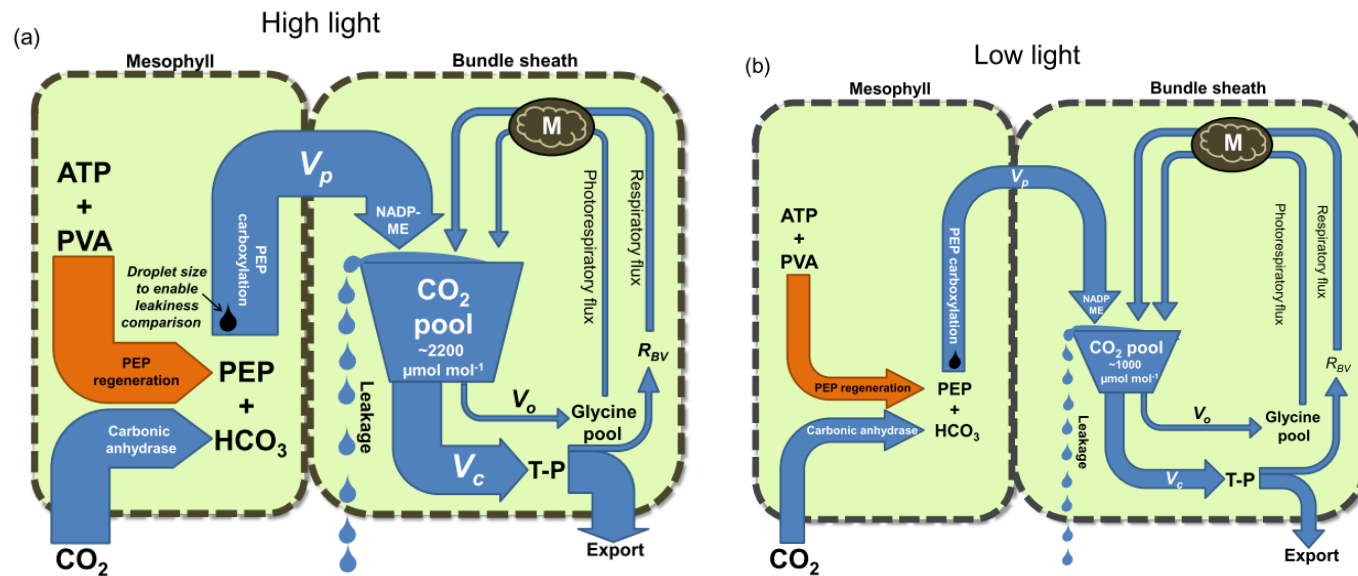


Figure B2. Reproduced from Sage et al., 2014. A schematic showing the flow of newly fixed carbon in a NADP-malic enzyme type of C4 leaf grown at high light, and then measured at (a) high light and (b) low light. Arrow widths approximate the relative carbon flow through the various stages of C4 photosynthesis (Bellasio & Griffiths 2013; Ubierna et al. 2013). M, mitochondria; NADP-ME, NADP-malic enzyme; PEP, phosphoenolpyruvate; PVA, pyruvate;  $R_{BV}$ , mitochondrial respiration rate in the bundle sheath and vascular bundle; T-P, triose-phosphate;  $V_c$ , RuBP carboxylation rate;  $V_p$ , PEP carboxylation rate;  $V_o$ , RuBP oxygenation rate. In the transition to low light (panel B), the pool size of  $\text{CO}_2$  in the bundle sheath (CBS) decreases due to the reduced flux of  $\text{CO}_2$  from the mesophyll cells (smaller  $V_p$ , as indicated by a narrower arrow). The flux out of the  $\text{CO}_2$  pool at low light is lowered due to reduced RuBP carboxylase activity by Rubisco, leading to reduced export of carbohydrate. The leakage out of the  $\text{CO}_2$  pool at low light is also reduced due to a less steep  $\text{CO}_2$  gradient between mesophyll and bundle sheath cells (smaller droplet size in b); however, leakiness, the leak rate (L) relative to  $V_p$ , would be greater (compare droplet sizes to the width of the respective  $V_p$  arrow). The greater photorespiratory flux ( $V_o$ ) also decreases at low light due to a reduced RuBP regeneration rate; however, because  $V_o/V_c$  rises at the lower CBS, the decline is less than the decline in  $V_p$  and  $V_c$ , which are assumed to be well coordinated. The respiration rate is assumed to be unchanged. Note that at low light, the slightly greater photorespiratory flux and the unchanged respiratory flux contribute proportionally more  $\text{CO}_2$  to the  $\text{CO}_2$  pool. This increased fractional contribution of (photo)respiratory carbon causes the greater leakiness observed at low light (Bellasio & Griffiths 2013; Ubierna et al. 2013).

**Table B1. Published data used in figures 17 and 18.**

Reference	Plant Species	Type	Photosynthetic pathway	Sample location	$^{2}\epsilon_{\text{lipid}} \text{C}_{29}$	$^{13}\epsilon_{\text{lipid}} \text{C}_{29}$
Bi et al. (2005)	<i>Bothriochloa ischaemum</i>	Grass	C <sub>4</sub>	Guangzhou, China	-98	-8.3
Bi et al. (2005)	<i>Imperata cylindrica</i>	Grass	C <sub>4</sub>	Guangzhou, China	-142	-8
Bi et al. (2005)	<i>Zea mays</i>	Grass	C <sub>4</sub>	Guangzhou, China	-115	-10.6
Bi et al. (2005)	<i>Zoysia japonica</i>	Grass	C <sub>4</sub>	Guangzhou, China	-85	-10.6
Chikaraishi & Naraoka (2003)	<i>Phragmites communis</i>	Grass	C <sub>3</sub>	Gunma, Japan	-152	-2.4
Chikaraishi & Naraoka (2003)	<i>Miscanthus sinensis</i>	Grass	C <sub>4</sub>	Gunma, Japan	-130	-6.4
Chikaraishi & Naraoka (2003)	<i>Saccharum officinarum</i>	Grass	C <sub>4</sub>	Okinawa, Japan	-156	-8.1
Chikaraishi & Naraoka (2003)	<i>Saccharum officinarum</i>	Grass	C <sub>4</sub>	Thailand	-139	-8.1
Chikaraishi & Naraoka (2003)	<i>Sorghum bicolor</i>	Grass	C <sub>4</sub>	Thailand	-136	-6.9
Chikaraishi & Naraoka (2003)	<i>Miscanthus sinensis</i>	Grass	C <sub>4</sub>	Tokyo, Japan	-131	-7.2
Chikaraishi & Naraoka (2003)	<i>Zea mays</i>	Grass	C <sub>4</sub>	Tokyo, Japan	-110	-8.3
Chikaraishi & Naraoka (2003)	<i>Zoysia japonica</i>	Grass	C <sub>4</sub>	Tokyo, Japan	-136	-10.7
Krull et al. (2006)	<i>Astrelia pectinata</i>	Grass	C <sub>4</sub>	Queensland, Australia	-168	-10.9
Krull et al. (2006)	<i>Iseilema</i> sp.	Grass	C <sub>4</sub>	Queensland, Australia	-134	-9.4
Smith and Freeman (2006)	<i>Bromus inermis</i>	Grass	C <sub>3</sub>	Boulder, CO, USA	-198	-13.5
Smith and Freeman (2006)	<i>Andropogon gerardii</i>	Grass	C <sub>4</sub>	Boulder, CO, USA	-159	-9.6
Smith and Freeman (2006)	<i>Agropyron smithii</i>	Grass	C <sub>3</sub>	Cottonwood, SD, USA	-174	-13.6
Smith and Freeman (2006)	<i>Bromus inermis</i>	Grass	C <sub>3</sub>	Cottonwood, SD, USA	-167	-12.1
Smith and Freeman (2006)	<i>Koeleria pyramidata</i>	Grass	C <sub>3</sub>	Cottonwood, SD, USA	-193	-11.5
Smith and Freeman (2006)	<i>Buchloe dactyloides</i>	Grass	C <sub>4</sub>	Cottonwood, SD, USA	-147	-15
Smith and Freeman (2006)	<i>Schizachyrium scoparium</i>	Grass	C <sub>4</sub>	Cottonwood, SD, USA	-162	-6.9
Smith and Freeman (2006)	<i>Agropyron smithii</i>	Grass	C <sub>3</sub>	Hays, KS, USA	-157	-13.2
Smith and Freeman (2006)	<i>Andropogon gerardii</i>	Grass	C <sub>4</sub>	Hays, KS, USA	-159	-11.4
Smith and Freeman (2006)	<i>Panicum virgatum</i>	Grass	C <sub>4</sub>	Hays, KS, USA	-158	-10.8
Smith and Freeman (2006)	<i>Sorghastrum nutans</i>	Grass	C <sub>4</sub>	Hays, KS, USA	-142	-11.5
Smith and Freeman (2006)	<i>Agropyron smithii</i>	Grass	C <sub>3</sub>	Mandan, ND, USA	-176	-16.1
Smith and Freeman (2006)	<i>Stipa comata</i>	Grass	C <sub>3</sub>	Mandan, ND, USA	-145	-12.4

Reference	Plant Species	Type	Photosynthetic pathway	Sample location	$^2\epsilon_{\text{lipid}} \text{C}_{29}$	$^{13}\epsilon_{\text{lipid}} \text{C}_{29}$
Smith and Freeman (2006)	<i>Stipa viridula</i>	Grass	C <sub>3</sub>	Mandan, ND, USA	-163	-11.6
Smith and Freeman (2006)	<i>Bouteloua gracilis</i>	Grass	C <sub>4</sub>	Mandan, ND, USA	-143	-14
Smith and Freeman (2006)	<i>Calamovilfa longifolia</i>	Grass	C <sub>4</sub>	Mandan, ND, USA	-139	-16.5
Smith and Freeman (2006)	<i>Schizachyrium scoparium</i>	Grass	C <sub>4</sub>	Mandan, ND, USA	-152	-9.2
Smith and Freeman (2006)	<i>Elymus canadensis</i>	Grass	C <sub>3</sub>	Manhattan, KS, USA	-189	-12.5
Smith and Freeman (2006)	<i>Poa pratensis</i>	Grass	C <sub>3</sub>	Manhattan, KS, USA	-174	-10.9
Smith and Freeman (2006)	<i>Andropogon gerardii</i>	Grass	C <sub>4</sub>	Manhattan, KS, USA	-158	-13.6
Smith and Freeman (2006)	<i>Schizachyrium scoparium</i>	Grass	C <sub>4</sub>	Manhattan, KS, USA	-149	-13.5
Smith and Freeman (2006)	<i>Sorghastrum nutans</i>	Grass	C <sub>4</sub>	Manhattan, KS, USA	-149	-9.9
Smith and Freeman (2006)	<i>Agropyron smithii</i>	Grass	C <sub>3</sub>	Nunn, CO, USA	-131	-14.3
Smith and Freeman (2006)	<i>Stipa comata</i>	Grass	C <sub>3</sub>	Nunn, CO, USA	-127	-8.4
Smith and Freeman (2006)	<i>Bouteloua gracilis</i>	Grass	C <sub>4</sub>	Nunn, CO, USA	-104	-13.1
Smith and Freeman (2006)	<i>Oryzopsis hymenoides</i>	Grass	C <sub>3</sub>	Socorro County, NM, USA	-119	-12.7
Smith and Freeman (2006)	<i>Stipa comata</i>	Grass	C <sub>3</sub>	Socorro County, NM, USA	-97	-10.8
Smith and Freeman (2006)	<i>Bouteloua eriopoda</i>	Grass	C <sub>4</sub>	Socorro County, NM, USA	-64	-16
Smith and Freeman (2006)	<i>Bouteloua gracilis</i>	Grass	C <sub>4</sub>	Socorro County, NM, USA	-123	-13.3
Smith and Freeman (2006)	<i>Bromus inermis</i>	Grass	C <sub>3</sub>	Woodworth, ND, USA	-204	-11.5
Smith and Freeman (2006)	<i>Poa pratensis</i>	Grass	C <sub>3</sub>	Woodworth, ND, USA	-173	-10.4
Smith and Freeman (2006)	<i>Schizachyrium scoparium</i>	Grass	C <sub>4</sub>	Woodworth, ND, USA	-146	-9.2
Bi et al. (2005)	<i>Alternanthera bettzickiana</i>	Herb	C <sub>3</sub>	Guangzhou, China	-176	-9.7
Bi et al. (2005)	<i>Alternanthera versicolor</i>	Herb	C <sub>3</sub>	Guangzhou, China	-178	-8.5
Bi et al. (2005)	<i>Amaranthus paniculatus</i>	Herb	C <sub>4</sub>	Guangzhou, China	-59	-11.6
Bi et al. (2005)	<i>Amaranthus tricolor.</i>	Herb	C <sub>4</sub>	Guangzhou, China	-88	-12.3
Chikaraishi & Naraoka (2003)	<i>Acer palmatum</i>	Herb	C <sub>3</sub>	Gunma, Japan	-114	-3.1
Chikaraishi & Naraoka (2003)	<i>Artemisia princeps</i>	Herb	C <sub>3</sub>	Gunma, Japan	-99	-4.4
Chikaraishi & Naraoka (2003)	<i>Manihot utilissima</i>	Herb	C <sub>3</sub>	Thailand	-98	-2.4
Chikaraishi & Naraoka (2003)	<i>Acer argutum</i>	Tree	C <sub>3</sub>	Gunma, Japan	-59	-1.8

Reference	Plant Species	Type	Photosynthetic pathway	Sample location	$^2\epsilon_{\text{lipid}}\text{C}_{29}$	$^{13}\epsilon_{\text{lipid}}\text{C}_{29}$
Chikaraishi & Naraoka (2003)	<i>Acer argutum</i>	Tree	C3	Gunma, Japan	-63	-0.8
Chikaraishi & Naraoka (2003)	<i>Acer carpinifolium</i>	Tree	C3	Gunma, Japan	-75	-3.8
Chikaraishi & Naraoka (2003)	<i>Acer carpinifolium</i>	Tree	C3	Gunma, Japan	-104	-3.6
Chikaraishi & Naraoka (2003)	<i>Taraxacum officinale</i>	Tree	C3	Gunma, Japan	-97	-4.4
Chikaraishi & Naraoka (2003)	<i>Benthamidia japonica</i>	Tree	C3	Gunma, Japan	-100	-2.3
Chikaraishi & Naraoka (2003)	<i>Benthamidia japonica</i>	Tree	C3	Gunma, Japan	-113	-3.3
Chikaraishi & Naraoka (2003)	<i>Quercus dentata</i>	Tree	C3	Gunma, Japan	-138	-2.7
Chikaraishi & Naraoka (2003)	<i>Quercus mongolica</i>	Tree	C3	Gunma, Japan	-132	-3.8
Chikaraishi & Naraoka (2003)	<i>Prunus jamasakura</i>	Tree	C3	Gunma, Japan	-127	-2.3
Chikaraishi & Naraoka (2003)	<i>Cryptomeria japonica</i>	Tree	C3	Gunma, Japan	-98	-6.1
Chikaraishi & Naraoka (2003)	<i>Cryptomeria japonica</i>	Tree	C3	Gunma, Japan	-111	-5.1
Chikaraishi & Naraoka (2003)	<i>Albizia julibrissin</i>	Tree	C3	Ogasawara, Japan	-88	-2.7
Chikaraishi & Naraoka (2003)	<i>Quercus acutissima</i>	Tree	C3	Tokyo, Japan	-102	-2.8
Chikaraishi & Naraoka (2003)	<i>Camellia sasanqua</i>	Tree	C3	Tokyo, Japan	-125	-2.8
Chikaraishi & Naraoka (2003)	<i>Chamaecyparis obtusa</i>	Tree	C3	Tokyo, Japan	-107	-2.4
Chikaraishi & Naraoka (2003)	<i>Pinus thunbergii</i>	Tree	C3	Tokyo, Japan	-122	-7.7
Krull et al. (2006)	<i>Atalaya hemiglauca</i>	Tree	C3	Queensland, Australia	-138	-9.2
Krull et al. (2006)	<i>Acacia</i> sp.	Tree	C3	Queensland, Australia	-96	-8

## References

- Albert B. Y., Chibnall C., Piper S. H., Pollard A., Williams E. F. and Sahai P. N. (1934) The Constitution of the primary alcohols, fatty acids and paraffins present in plant and insect waxes. *Biogeochemistry* **28**, 2189–2208.
- Amelung W. and Brodowski S. (2008) Combining Biomarker with Stable Isotope Analyses for Assessing the Transformation and Turnover of Soil Organic Matter. In *Advances in Agronomy* Elsevier Inc. pp. 155–250.
- Aranibar J. N., Berry J. a., Riley W. J., Pataki D. E., Law B. E. and Ehleringer J. R. (2006) Combining meteorology, eddy fluxes, isotope measurements, and modeling to understand environmental controls of carbon isotope discrimination at the canopy scale. *Glob. Chang. Biol.* **12**, 710–730.
- Bassham J. A., Benson A. A. and Calvin M. (1950) The path of carbon in photosynthesis: the role of malic acid. *J. Biol. Chem.*, 781–787.
- Bellasio C. and Griffiths H. (2014) Acclimation to low light by C4 maize: implications for bundle sheath leakiness. *Plant. Cell Environ.* **37**, 1046–58.
- Bi X., Sheng G., Liu X., Li C. and Fu J. (2005) Molecular and carbon and hydrogen isotopic composition of n-alkanes in plant leaf waxes. *Org. Geochem.* **36**, 1405–1417.
- Boom a., Carr a. S., Chase B. M., Grimes H. L. and Meadows M. E. (2014) Leaf wax n-alkanes and  $\delta^{13}\text{C}$  values of CAM plants from arid southwest Africa. *Org. Geochem.* **67**, 99–102.
- Boot C. S., Ettwein V. J., Maslin M. a., Weyhenmeyer C. E. and Pancost R. D. (2006) A 35,000 year record of terrigenous and marine lipids in Amazon Fan sediments. *Org. Geochem.* **37**, 208–219.
- Bourdenx B., Bernard A., Domergue F., Pascal S., Léger A., Roby D., Pervent M., Vile D., Haslam R. P., Napier J. a, Lessire R. and Joubès J. (2011) Overexpression of Arabidopsis ECERIFERUM1 promotes wax very-long-chain alkane biosynthesis and influences plant response to biotic and abiotic stresses. *Plant Physiol.* **156**, 29–45.
- Bowen G. J. and Revenaugh J. (2003) Interpolating the isotopic composition of modern meteoric precipitation. *Water Resour. Res.* **39**, n/a–n/a.
- Bowling D., McDowell N., Bond B., Law B. and Ehleringer J. (2002)  $^{13}\text{C}$  content of ecosystem respiration is linked to precipitation and vapor pressure deficit. *Oecologia* **131**, 113–124.
- Buchmann N., Brooks J. R., Rapp K. D. and Ehleringer J. R. (1996) Carbon isotope composition of C4 grasses is influenced by light and water supply. *Plant. Cell Environ.*, 392–402.

- Buchmann N., Kao W.-Y. and Ehleringer J. (1997) Influence of stand structure on carbon-13 of vegetation, soils, and canopy air within deciduous and evergreen forests in Utah, United States. *Oecologia* **110**, 109–119.
- Burgoyne T. W. and Hayes J. M. (1998) Quantitative Production of H<sub>2</sub> by Pyrolysis of Gas Chromatographic Effluents. *Anal. Chem.* **70**, 5136–5141.
- Bush R. T. and McInerney F. a (2015) Influence of temperature and C<sub>4</sub> abundance on n-alkane chain length distributions across the central USA. *Org. Geochem.* **79**, 65–73.
- Bush R. T. and McInerney F. a. (2013) Leaf wax n-alkane distributions in and across modern plants: Implications for paleoecology and chemotaxonomy. *Geochim. Cosmochim. Acta* **117**, 161–179.
- Carr A. S., Boom A., Grimes H. L., Chase B. M., Meadows M. E. and Harris A. (2014) Leaf wax n-alkane distributions in arid zone South African flora: Environmental controls, chemotaxonomy and palaeoecological implications. *Org. Geochem.* **67**, 72–84.
- Cerling T. E., Harris J. M., Macfadden B. J., Leakey M. G., Quade J., Eisenmann V. and Ehleringer J. R. (1997) Global vegetation change through the Miocene / Pliocene boundary. , 153–158.
- Cernusak L. A., Ubierna N., Winter K., Holtum J. A. M., Marshall J. D. and Farquhar G. D. (2013) Tansley review Environmental and physiological determinants of carbon isotope discrimination in terrestrial plants.
- Chadwick O. a., Gavenda R. T., Kelly E. F., Ziegler K., Olson C. G., Elliott W. C. and Hendricks D. M. (2003) The impact of climate on the biogeochemical functioning of volcanic soils. *Chem. Geol.* **202**, 195–223.
- Chadwick O. a., Kelly E. F., Hotchkiss S. C. and Vitousek P. M. (2007) Precontact vegetation and soil nutrient status in the shadow of Kohala Volcano, Hawaii. *Geomorphology* **89**, 70–83.
- Chikaraishi Y. and Naraoka H. (2003) Compound-specific  $\delta\text{D}$ – $\delta^{13}\text{C}$  analyses of n-alkanes extracted from terrestrial and aquatic plants. *Phytochemistry* **63**, 361–371.
- Chikaraishi Y., Naraoka H. and Poulson S. R. (2004) Hydrogen and carbon isotopic fractionations of lipid biosynthesis among terrestrial (C<sub>3</sub>, C<sub>4</sub> and CAM) and aquatic plants. *Phytochemistry* **65**, 1369–81.
- Collister J. W., Rieley G., Stern B., Eglinton G. and Fry B. (1994) Compound-specific delta <sup>13</sup>C analyses of leaf lipids from plants with differing carbon dioxide metabolisms. *Org. Geochem.* **21**, 619–627.
- Cusack D. F., Chadwick O. a., Ladefoged T. and Vitousek P. M. (2012) Long-term effects of agriculture on soil carbon pools and carbon chemistry along a Hawaiian environmental gradient. *Biogeochemistry* **112**, 229–243.

- Van D Water P. K., Leavitt S. W. and Betancourt J. L. (2002) Leaf  $\delta^{13}\text{C}$  variability with elevation, slope aspect, and precipitation Leaf  $\delta^{13}\text{C}$  variability in the southwest United States. *Oecologia* **132**, 332–343.
- Daehler C. C. and Goergen E. M. (2005) Experimental Restoration of an Indigenous Hawaiian Grassland after Invasion by Buffel Grass (*Cenchrus ciliaris*). *Restor. Ecol.* **13**, 380–389.
- Darrouzet-nardi A., Antonio C. M. D. and Dawson T. E. (2006) Depth of water acquisition by invading shrubs and resident herbs in a Sierra Nevada meadow. , 31–43.
- Dawson T. E. (1996) Determining water use by trees and forests from isotopic, energy balance and transpiration analyses: the roles of tree size and hydraulic lift. *Tree Physiol.* **16**, 263–272.
- Deniro M. J. and Epstein S. (1977) Mechanism of Carbon Isotope Fractionation Associated with Lipid Synthesis Mechanism of Carbon Isotope Fractionation Associated with Lipid Synthesis. *Science* (80-. ). **197**, 261–263.
- Diefendorf A. F. (2010) Environmental and Ecological Constraints on Molecular and Isotopic Signatures in Terrestrial Organic Carbon. .
- Diefendorf A. F., Freeman K. H. and Wing S. L. (2014) A comparison of terpenoid and leaf fossil vegetation proxies in Paleocene and Eocene Bighorn Basin sediments. *Org. Geochem.* **71**, 30–42.
- Diefendorf A. F., Freeman K. H., Wing S. L. and Graham H. V. (2011) Production of n-alkyl lipids in living plants and implications for the geologic past. *Geochim. Cosmochim. Acta* **75**, 7472–7485.
- Diefendorf A. F., Mueller K. E., Wing S. L., Koch P. L. and Freeman K. H. (2010) Global patterns in leaf  $^{13}\text{C}$  discrimination and implications for studies of past and future climate. *Proc. Natl. Acad. Sci. U. S. A.* **107**, 5738–43.
- Domínguez E., Cuartero J. and Heredia A. (2011) An overview on plant cuticle biomechanics. *Plant Sci.* **181**, 77–84.
- Dupont L. M., Rommerskirchen F., Mollenhauer G. and Schefuß E. (2013) Miocene to Pliocene changes in South African hydrology and vegetation in relation to the expansion of C4 plants. *Earth Planet. Sci. Lett.* **375**, 408–417.
- Edwards E. J., Osborne C. P., Strömberg C. a E., Smith S. a, Bond W. J., Christin P.-A., Cousins A. B., Duvall M. R., Fox D. L., Freckleton R. P., Ghannoum O., Hartwell J., Huang Y., Janis C. M., Keeley J. E., Kellogg E. a, Knapp A. K., Leakey A. D. B., Nelson D. M., Saarela J. M., Sage R. F., Sala O. E., Salamin N., Still C. J. and Tiplle B. (2010) The origins of C4 grasslands: integrating evolutionary and ecosystem science. *Science* **328**, 587–91.

- Edwards E. J. and Smith S. a (2010) Phylogenetic analyses reveal the shady history of C<sub>4</sub> grasses. *Proc. Natl. Acad. Sci. U. S. A.* **107**, 2532–7.
- Eglinton G., Gonzalez A., Hamilton R. and Raphael R. A. (1962) Hydrocarbon constituents of the wax coating of plant leaves: a taxonomic survey. *Phytochemistry* **1**, 89–102.
- Eglinton G. and Hamilton R. (1967) Leaf epicuticular waxes. *Science (80- )*. **156**, 1322–1335.
- Ehleringer J. R. (1978) Implications of Quantum Yield Differences on the Distributions of C<sub>3</sub> and C<sub>4</sub> Grasses. *Int. Assoc. Ecol.* **31**, 255–267.
- Ehleringer J. R., Cerling T. E. and Helliker B. R. (1997) C<sub>4</sub> photosynthesis , Atmospheric CO<sub>2</sub>, and Climate. **112**, 285–299.
- Ehleringer J. R. and Dawson T. E. (1992) Water uptake by plants: perspectives from stable isotope composition. *Plant, Cell Environ.* **15**, 1073–1082.
- Ehleringer J. R., Sage R. F., Flanagan L. B. and Pearcy R. W. (1991) Climate change and the evolution of C(4) photosynthesis. *Trends Ecol. Evol.* **6**, 95–9.
- El-hajj Z., Kavanagh K., Rose C. and Kanaan-atallah Z. (2004) Nitrogen and carbon dynamics of a foliar biotrophic fungal parasite in fertilized Douglas-fir. *New Phytol.* **163**, 139–148.
- Farquhar G. D., Ehleringer J. R. and Hubick K. T. (1989) Carbon Isotope Discrimination and Photosynthesis. *Annu. Rev. Plant Physiol. Plant Mol. Biol.* **40**, 503–537.
- Feakins S. J. and Sessions A. L. (2010) Controls on the D/H ratios of plant leaf waxes in an arid ecosystem. *Geochim. Cosmochim. Acta* **74**, 2128–2141.
- Feng X. (1999) Trends in intrinsic water-use efficiency of natural trees for the past 100 –200 years: A response to atmospheric CO<sub>2</sub> concentration. *Geochim. Cosmochim. Acta* **63**, 1891–1903.
- Freeman K. H. and Colarusso L. (2001) Molecular and isotopic records of C<sub>4</sub> grassland expansion in the late Miocene. *Geochim. Cosmochim. Acta* **65**, 1439–1454.
- Freeman K. H. and Pancost R. D. (2014) *Biomarkers for Terrestrial Plants and Climate*. 2nd ed., Elsevier Ltd.
- Gagosian R. B. (1986) The importance of atmospheric input of terrestrial material to deep sea sediments \* organic.
- Gagosian R. and Peltzer E. (1986) The importance of atmospheric input of terrestrial organic material to deep sea sediments. *Org. Geochem.* **325**, 800–804.



- Galy V., Eglinton T., France-Lanord C. and Sylva S. (2011) The provenance of vegetation and environmental signatures encoded in vascular plant biomarkers carried by the Ganges–Brahmaputra rivers. *Earth Planet. Sci. Lett.* **304**, 1–12.
- Ghannoum O., Paul M. J., Ward J. L., Beale M. H., Corol D.-I. and Conroy J. P. (2008) The sensitivity of photosynthesis to phosphorus deficiency differs between C 3 and C 4 tropical grasses. *Funct. Plant Biol.* **35**, 213.
- Graham H. V (2014) Molecular and Isotopic Indicators of Canopy Closure in Ancient Forests and the Effects of Environmental Gradients on Leaf Alkane Expression. .
- Gröcke D. R. (2002) The carbon isotope composition of ancient CO<sub>2</sub> based on higher-plant organic matter. *Philos. Trans. A. Math. Phys. Eng. Sci.* **360**, 633–58.
- Hayes J. M., Freeman K. H., Popp B. N. and Hoham C. H. (1990) Compound-specific isotopic analyses: a novel tool for reconstruction of ancient biogeochemical processes. *Org. Geochem.* **16**, 1115–28.
- Henderson A. K., Graham H., Magill C. R., Fox D., Patzkowsky M. E. and Freeman K. H. (2014) Angiosperm n-alkane distribution patterns and the geologic record of C 4 grasslands. *Geochim. Cosmochim. Acta.*
- Hobbie E, SA M. and HH S. (2014) Insights into nitrogen and carbon dynamics of ectomycorrhizal and saprotrophic fungi from isotopic evidence. *Oecologia* **118**, 353–360.
- Hren M. T., Pagani M., Erwin D. M. and Brandon M. (2010) Biomarker reconstruction of the early Eocene paleotopography and paleoclimate of the northern Sierra Nevada. *Geology* **38**, 7–10.
- Keeling C. D. (1958) The concentration and isotopic abundances of atmospheric carbon dioxide in rural areas. *Geochim. Cosmochim. Acta* **13**, 322–334.
- Kerstiens G. (1996) Cuticular water permeability and its physiological significance. **47**, 1813–1832.
- Krishnamurthy R. V, Syrup K. a, Baskaran M. and Long a (1995) Late glacial climate record of midwestern United States from the hydrogen isotope ratio of lake organic matter. *Science* **269**, 1565–7.
- Krull E., Sachse D., Mügler I., Thiele A. and Gleixner G. (2006) Compound-specific  $\delta^{13}\text{C}$  and  $\delta^2\text{H}$  analyses of plant and soil organic matter: A preliminary assessment of the effects of vegetation change on ecosystem hydrology. *Soil Biol. Biochem.* **38**, 3211–3221.
- Lanigan G. J., Betson N., Griffiths H. and Seibt U. (2008) Carbon isotope fractionation during photorespiration and carboxylation in Senecio. *Plant Physiol.* **148**, 2013–2020.
- Leider A., Hinrichs K.-U., Schefuß E. and Versteegh G. J. M. (2013) Distribution and stable isotopes of plant wax derived n-alkanes in lacustrine, fluvial and marine surface sediments

- along an Eastern Italian transect and their potential to reconstruct the hydrological cycle. *Geochim. Cosmochim. Acta* **117**, 16–32.
- Lopes dos Santos R. a., De Deckker P., Hopmans E. C., Magee J. W., Mets A., Sinninghe Damsté J. S. and Schouten S. (2013) Abrupt vegetation change after the Late Quaternary megafaunal extinction in southeastern Australia. *Nat. Geosci.* **6**, 627–631.
- Ma J.-Y., Sun W., Liu X.-N. and Chen F.-H. (2012) Variation in the stable carbon and nitrogen isotope composition of plants and soil along a precipitation gradient in northern China. *PLoS One* **7**, e51894.
- Macková J., Vašková M., Macek P., Hronková M., Schreiber L. and Šantrůček J. (2013) Plant response to drought stress simulated by ABA application: Changes in chemical composition of cuticular waxes. *Environ. Exp. Bot.* **86**, 70–75.
- Maffei M. (1996) Chemotaxonomic Significance of Leaf Wax Alkanes in the Gramineae Wax alkanes represent an interesting portion of wax coatings and recently the Solanaceae ( Zygadlo et al , 1994 ), Crassulaceae ( Stevens et al , 1994 ), Labiatae and references cited therei. *Biochem. Syst. Ecol.* **24**, 53–64.
- Magill C. R., Ashley G. M. and Freeman K. H. (2013a) Ecosystem variability and early human habitats in eastern Africa. *Proc. Natl. Acad. Sci. U. S. A.* **110**, 1167–74.
- Magill C. R., Ashley G. M. and Freeman K. H. (2013b) Water, plants, and early human habitats in eastern Africa. *Proc. Natl. Acad. Sci. U. S. A.* **110**, 1175–80.
- McCoy M. D., Browne Ribeiro A. T., Graves M. W., Chadwick O. a. and Vitousek P. M. (2013) Irrigated taro (*Colocasia esculenta*) farming in North Kohala, Hawai‘i: sedimentology and soil nutrient analyses. *J. Archaeol. Sci.* **40**, 1528–1538.
- McInerney F. A., Freeman K. H., Polissar P. J. and Feakins S. J. (2013) Environmental and biosynthetic influences on carbon and hydrogen isotope ratios of leaf wax. *Am. Geophys. Union Annu. Meet.*
- McInerney F. a., Helliker B. R. and Freeman K. H. (2011) Hydrogen isotope ratios of leaf wax n-alkanes in grasses are insensitive to transpiration. *Geochim. Cosmochim. Acta* **75**, 541–554.
- Meyers P. A. and Ishiwatari R. (1993) Lacustrine organic geochemistryman overview of indicators of organic matter sources and diagenesis in lake sediments. **20**, 867–900.
- Monson K. D. and Hayes J. M. (1982) Carbon isotopic fractionation in the biosynthesis of bacterial fatty acids . Ozonolysis of unsaturated fatty acids as a means of determining the intramolecular distribution of carbon isotopes. *Geochim. Cosmochim. Acta* **46**, 139–149.
- Muscolo a., Panuccio M. R. and Eshel a. (2013) Ecophysiology of *Pennisetum clandestinum*: a valuable salt tolerant grass. *Environ. Exp. Bot.* **92**, 55–63.
- O’Leary M. (1981) Carbon Isotope Fractionation in Plants. *Phytochemistry* **20**, 553–567.

- O'Leary M. (1988) Carbon Isotopes in Photosynthesis. *Bioscience* **38**, 328–336.
- Pancost R. D., Freeman K. H., Herrmann A. D., Patzkowsky M. E., Ainsaar L. and Martma T. (2013) Reconstructing Late Ordovician carbon cycle variations. *Geochim. Cosmochim. Acta* **105**, 433–454.
- Pataki D. E. (2003) The application and interpretation of Keeling plots in terrestrial carbon cycle research. *Global Biogeochem. Cycles* **17**.
- Pau S., Edwards E. J. and Still C. J. (2013) Improving our understanding of environmental controls on the distribution of C3 and C4 grasses. *Glob. Chang. Biol.* **19**, 184–96.
- Pearcy R. W. and Ehleringer J. (1984) Comparative ecophysiology of C3 and C4 plants. *Plant, Cell Environ.* **7**, 1–13.
- Pedentchouk N., Sumner W., Tipple B. and Pagani M. (2008)  $\delta^{13}\text{C}$  and  $\delta\text{D}$  compositions of n-alkanes from modern angiosperms and conifers: An experimental set up in central Washington State, USA. *Org. Geochem.* **39**, 1066–1071.
- Polissar P. J. and D'Andrea W. J. (2014) Uncertainty in paleohydrologic reconstructions from molecular  $\delta\text{D}$  values. *Geochim. Cosmochim. Acta* **129**, 146–156.
- Prentice I. C., Meng T., Wang H., Harrison S. P., Ni J. and Wang G. (2011) Evidence of a universal scaling relationship for leaf  $\text{CO}_2$  drawdown along an aridity gradient. *New Phytol.* **190**, 169–80.
- Rao B., Li B., Oosterhuist D. M., Murphy J. B. and Kim K. S. O. O. (1996) EFFECT OF WATER STRESS ON THE EPICUTICULAR WAX COMPOSITION AND ULTRASTRUCTURE OF COTTON ( *GOSSYPIMUM HIRSUTUM* L .) LEAF , BRACT , AND BOLL. *Environ. Exp. Bot.* **36**, 61–69.
- Rommerskirchen F., Eglinton G., Dupont L. and Rullkötter J. (2006) Glacial/interglacial changes in southern Africa: Compound-specific  $\delta^{13}\text{C}$  land plant biomarker and pollen records from southeast Atlantic continental margin sediments. *Geochemistry, Geophys. Geosystems* **7**, n/a–n/a.
- Rommerskirchen F., Plader A., Eglinton G., Chikaraishi Y. and Rullkötter J. (2006) Chemotaxonomic significance of distribution and stable carbon isotopic composition of long-chain alkanes and alkan-1-ols in C4 grass waxes. *Org. Geochem.* **37**, 1303–1332.
- Rundel P. W. (1980) The Ecological Distribution of C3 and C4 Grasses in the Hawaiian Islands. **45**, 354–359.
- Sachse D., Billault I., Bowen G. J., Chikaraishi Y., Dawson T. E., Feakins S. J., Freeman K. H., Magill C. R., McInerney F. a., van der Meer M. T. J., Polissar P., Robins R. J., Sachs J. P., Schmidt H.-L., Sessions A. L., White J. W. C., West J. B. and Kahmen A. (2012) Molecular Paleohydrology: Interpreting the Hydrogen-Isotopic Composition of Lipid Biomarkers from Photosynthesizing Organisms. *Annu. Rev. Earth Planet. Sci.* **40**, 221–249.

- Sachse D., Dawson T. E. and Kahmen A. (2015) Seasonal variation of leaf wax n-alkane production and  $\delta^2\text{H}$  values from the evergreen oak tree, *Quercus agrifolia*. *Isotopes Environ. Health Stud.*, 1–19.
- Sachse D., Radke J. and Gleixner G. (2006)  $\delta\text{D}$  values of individual n-alkanes from terrestrial plants along a climatic gradient – Implications for the sedimentary biomarker record. *Org. Geochem.* **37**, 469–483.
- Sage R. F. (2014) Stopping the leaks: new insights into C<sub>4</sub> photosynthesis at low light. *Plant. Cell Environ.* **37**, 1037–1041.
- Sage R. F. (2004) The evolution of C<sub>4</sub> photosynthesis. **161**, 341–370.
- Sage R. F. and McKown A. D. (2006) Is C<sub>4</sub> photosynthesis less phenotypically plastic than C<sub>3</sub> photosynthesis? *J. Exp. Bot.* **57**, 303–17.
- Scheiter S., Higgins S. I., Osborne C. P., Bradshaw C., Lunt D., Ripley B. S., Taylor L. L. and Beerling D. J. (2012) Fire and fire-adapted vegetation promoted C<sub>4</sub> expansion in the late Miocene. *New Phytol.* **195**, 653–66.
- Schimmelmann A., Sessions A. L. and Mastalerz M. (2006) Hydrogen Isotopic (D/H) Composition of Organic Matter During Diagenesis and Thermal Maturation. *Annu. Rev. Earth Planet. Sci.* **34**, 501–533.
- Scholl M. a., Ingebritsen S. E., Janik C. J. and Kauahikaua J. P. (1995) AN ISOTOPE HYDROLOGY STUDY OF THE KILAUEA VOLCANO AREA, HAWAII U. S. GEOLOGICAL SURVEY Water-Resources Investigations Report 95-4213. *U.S. Geol. Surv.*
- Scholl M. a., Ingebritsen S. E., Janik C. J. and Kauahikaua J. P. (1996) Use of Precipitation and Groundwater Isotopes to Interpret Regional Hydrology on a Tropical Volcanic Island: Kilauea Volcano Area, Hawaii. *Water Resour. Res.* **32**, 3525–3537.
- Schouten S., Woltering M., Rijpstra W. I. C., Sluijs A., Brinkhuis H. and Sinninghe Damsté J. S. (2007) The Paleocene–Eocene carbon isotope excursion in higher plant organic matter: Differential fractionation of angiosperms and conifers in the Arctic. *Earth Planet. Sci. Lett.* **258**, 581–592.
- Schwab V. F., Garcin Y., Sachse D., Todou G., Séné O., Onana J., Achoundong G. and Gleixner G. (2015) Effect of aridity on  $\delta^{13}\text{C}$  and  $\delta\text{D}$  values of C<sub>3</sub> plant- and C<sub>4</sub> graminoid-derived leaf wax lipids from soils along an environmental gradient in Cameroon (Western Central Africa). *Org. Geochem.* **78**, 99–109.
- Schwark L., Zink K. and Lechterbeck J. (2002) Reconstruction of postglacial to early Holocene vegetation history in terrestrial Central Europe via cuticular lipid biomarkers and pollen records from lake sediments. *Geology* **30**, 463.

- Silveria L. D., Sternberg L., Mulkey S. S. and Wright S. J. (1989) Ecological interpretation of leaf carbon isotope ratios: influence of respired carbon dioxide. *Ecology* **70**, 1317–1324.
- Smith F. a. and Freeman K. H. (2006) Influence of physiology and climate on  $\delta D$  of leaf wax n-alkanes from C3 and C4 grasses. *Geochim. Cosmochim. Acta* **70**, 1172–1187.
- Smith F., Wing S. and Freeman K. (2007) Magnitude of the carbon isotope excursion at the Paleocene–Eocene thermal maximum: The role of plant community change. *Earth Planet. Sci. Lett.* **262**, 50–65.
- Stewart G. R., Turnbull M. H., Schmidt S. and Erskine P. D. (1995)  $^{13}C$  Natural Abundance in Plant Communities Along a Rainfall Gradient : a Biological Integrator of Water Availability. *J. Plant Physiol.* **22**, 51–55.
- Still C. J., Berry J. a., Collatz G. J. and DeFries R. S. (2003) Global distribution of C3 and C4 vegetation: Carbon cycle implications. *Global Biogeochem. Cycles* **17**, 6–16–14.
- Sun Q., Xie M., Shi L., Zhang Z., Lin Y., Shang W., Wang K., Li W., Liu J. and Chu G. (2013) Alkanes, compound-specific carbon isotope measures and climate variation during the last millennium from varved sediments of Lake Xiaolongwan, northeast China. *J. Paleolimnol.* **50**, 331–344.
- Teeri A. J. A., Stowe L. G. and Url S. (2014) Climatic Patterns and the Distribution of C4 Grasses in North America. *Int. Assoc. Ecol.* **23**, 1–12.
- Tieszen L. L., Senyimba M. M., Imbamba S. K., Troughton J. H. and Url S. (1979) The Distribution of C3 and C4 Grasses and Carbon Isotope Discrimination along an Altitudinal and Moisture Gradient in Kenya. **37**, 337–350.
- Tipple B. J., Berke M. a, Doman C. E., Khachatryan S. and Ehleringer J. R. (2013) Leaf-wax n-alkanes record the plant-water environment at leaf flush. *Proc. Natl. Acad. Sci. U. S. A.* **110**, 2659–64.
- Tipple B. J. and Pagani M. (2010) A 35Myr North American leaf-wax compound-specific carbon and hydrogen isotope record: Implications for C4 grasslands and hydrologic cycle dynamics. *Earth Planet. Sci. Lett.* **299**, 250–262.
- Troughton J. H. and Card K. a (1975) Temperature effects on the carbon-isotope ratio of C3, C4 and crassulacean-acid-metabolism (CAM) plants. *Planta* **123**, 185–90.
- Ubierna N., Sun W., Kramer D. M. and Cousins A. B. (2013) The efficiency of C4 photosynthesis under low light conditions in *Zea mays*, *Miscanthus x giganteus* and *Flaveria bidentis*. *Plant, Cell Environ.* **36**, 365–381.
- Vogan P. J. and Sage R. F. (2012) Effects of low atmospheric CO2 and elevated temperature during growth on the gas exchange responses of C3, C3-C4 intermediate, and C4 species from three evolutionary lineages of C4 photosynthesis. *Oecologia* **169**, 341–52.

- Vogts A., Moossen H., Rommerskirchen F. and Rullkötter J. (2009) Distribution patterns and stable carbon isotopic composition of alkanes and alkan-1-ols from plant waxes of African rain forest and savanna C3 species. *Org. Geochem.* **40**, 1037–1054.
- Vogts A., Schefuß E., Badewien T. and Rullkötter J. (2012) n-Alkane parameters from a deep sea sediment transect off southwest Africa reflect continental vegetation and climate conditions. *Org. Geochem.* **47**, 109–119.
- Wei K. and Jia G. (2009) Soil n -alkane  $\delta^{13}\text{C}$  along a mountain slope as an integrator of altitude effect on plant species  $\delta^{13}\text{C}$ . *Geophys. Res. Lett.* **36**, L11401.
- Wilén C. a. and Holt J. S. (1996) Physiological mechanisms for the rapid growth of *Pennisetum clandestinum* in Mediterranean climates. *Weed Res.* **36**, 213–225.
- Zachos J. C., McCarren H., Murphy B., Röhl U. and Westerhold T. (2010) Tempo and scale of late Paleocene and early Eocene carbon isotope cycles: Implications for the origin of hyperthermals. *Earth Planet. Sci. Lett.* **299**, 242–249.